SIMULATION STUDY FOR IMPROVING SEAWATER POLYMER FLOOD PERFORMANCE IN STRATIFIED HIGH TEMPERATURE RESERVOIRS

A Thesis

by

GENG NIU

Submitted to the Office of Graduate and Professional Studies of
Texas A&M University
in partial fulfillment of the requirements for the degree of

MASTER OF SCIENCE

Chair of Committee,	Hisham A. Nasr-El-Din
Committee Members,	Robert H. Lane
	Mahmoud El-Halwagi
Head of Department,	A. Daniel Hill

December 2014

Major Subject: Petroleum Engineering

ABSTRACT

Polymer flood has achieved technical and commercial success, especially for its large-scale application in the Daqing oilfield in China. However, previous field tests indicated polymer flood was not economically successful for high temperature reservoirs when injected with high salinity, high hardness water. Novel thermal and salinity-resistance polymers have been developed, and their properties are tested via comprehensive lab experiments, which encourage further development of polymer flooding in high-temperature and high-salinity reservoirs.

To achieve a promising recovery effect, numerical simulation, including all significant physicochemical phenomena, must be carried out before field implementation to realize the reservoir response to polymer. An optimized recovery design, which minimizes costs and increases the process efficiency, should be proposed for reservoir models representing real harsh conditions including severe heterogeneity.

In this work, the effects of shear thinning, thermal thinning, degradation of polymer/seawater solution to oil recovery performance in stratified reservoir are studied in various temperature conditions. Also supporting measures for polymer flood, such as mechanical water shutoff and in-depth profile control, are studied to evaluate their ability in harsh reservoir conditions. Thermal thinning and shear thinning properties of polymer/seawater solution were measured by a rheometer, and compared with published data. Degradation and adsorption properties of the polymers, as well as the gelation

reaction and resistance properties of the gel were summarized from literature review generating reasonable parameters for simulation.

Simulation results indicate that thermal thinning of polymers has a marginal effect on the final oil recovery. Another property related to temperature, polymer thermal degradation, is obviously influenced by temperature, leading to decrease of the final oil recovery to different extent. Both water shutoff and in-depth profile control can improve waterflood. However deep profile control will be more efficient if polymer flood is applied, and the combination of in-depth profile control and polymer flood carried out with low injection temperature achieve the best recovery performance.

DEDICATION

To my parents.

ACKNOWLEDGEMENTS

I would like to thank my committee chair, Dr. Nasr-El-Din, for his support and guidance throughout my Master's in the Department of Petroleum Engineering. His patience, encouragement, and dedication to his work provided the energy for me to work hard on several projects during the last four years. In addition, I would like to thank my committee members, Dr. Lane and Dr. El-Halwagi, for their patience and support throughout the course of this research.

Thanks also goes to my friends and colleagues and the department faculty and staff for making my time at Texas A&M University a great experience. I also want to extend my gratitude to CMG, who provided the technical support.

Finally, I would like to give thanks to my mother and father for their encouragement and support and to my girlfriend for her patience and love.

NOMENCLATURE

EOR	Enhanced Oil Recovery
CMG	Computer Modelling Group

TABLE OF CONTENTS

Page

Page

LIST OF FIGURES

Page

Page

Page

LIST OF TABLES

Page

1. INTRODUCTION

1.1 Oil Recovery

Oil recovery processes are classified as primary recovery or primary depletion, secondary recovery or improved oil recovery (IOR), and tertiary recovery or enhanced oil recovery (EOR) (Gaillard et al. 2010). The driving force for primary recovery is natural energy. Its source includes bottom and edge water, solution gas, gas cap, and gravity. After primary recovery, for a while, natural energy will deplete and oil production will decline. Therefore the primary recovery is also called primary depletion. At this time, water or gas are injected to increase the energy of the reservoir, known as the secondary recovery. Waterflood is more popular due to its availability and efficiency.

Even after extensive secondary recovery, large amounts of oil are still uncovered due to reservoir heterogeneity and trapping. Tertiary recovery or EOR involves the injection of gas, chemicals, hot water, or steam to recover the remaining oil. The injected fluids enlarge the sweep efficiency, decrease the mobility ratio, and/or decrease the residual oil saturation.

Polymers are used in EOR to control the mobility ratio between the displaced fluid and displacing fluids as its main purpose. Polymer flood is now considered to be a technical and commercial success, especially since its large-scale application in Daqing oilfield in China, resulting in about 300,000 barrels of incremental oil per day (Wang et al. 2001). However there is a controversy about whether the polymer flood is an EOR

process or not. The fundamental feature of EOR distinguished from IOR is that it can significantly decrease the residual oil saturation. The conventional wisdom is that polymer does not reduce the residual oil saturation, because injection of polymer solution normally does not increase the capillary number enough to reduce the residual oil saturation under field conditions (Lake 2010). However, recent experiments (Wreath 1989; Lu 1994; Wang et al. 2001; Huh and Pope 2008) and field data (Putz et al. 1988; Wang et al. 2001; Xia et al. 2004) show the reduction of residual oil saturation caused by viscoelasticity of polymer also contribute to increment in oil recovery, even though this effect is not significant according to micro-scale experimental studies (Afsharpoor et al. 2014). In this study, the classification of polymer flood is not considered, and the viscoelasticity of polymer and gel is neglected.

1.2 History of Polymer Flood in High Temperature Condition

A synthetic water-soluble polymer, hydrolyzed polyacrylamide (HPAM) is widely used for polymer flood at moderate reservoir conditions, resulting in an incremental oil recovery factor of 10%-15% (Liu et al. 2009). When HPAM hydrolyzes in water, the negative charges in the carboxylate groups along the polyacrylamide chain make the chain stretch due to electrostatic repulsion (Nasr-El-Din et al. 1991; Lee et al. 2009). The extended polyacrylamide chain will enhance the viscosity of the displacing fluid, which also inhibits the physical entanglement of the solvated chains (Khan et al. 2009). Also, HPAM is feasible for reservoirs with temperatures as high as 100˚C if the concentration of Ca^{2+} is kept below 200 mg/L (Ikegami and Imai 1962). But HPAM degrades at high

temperature and will precipitate if excessive multivalent cations are present (Zaitoun and Potie 1983), leading to loss of viscosity enhancement. Although there are four main types of degradations affecting the viscosity (thermal, free radical, mechanical, and biological degradation), only thermal degradation is explored in this study.

Polyacrylamide (PAM) can be modified with various functional monomers to protect them from degradation. The anionic monomer, 2-acrylamido-2-methylpropane sulfonate (AMPS), also named acrylamido-tertiary-butyl sulfonate (ATBS), will help the polymers increase their tolerance to salinity and divalent ions by substituting some of the AM moieties (Levitt and Pope 2008). Such copolymer can also tolerate temperature to a certain extent in seawater (Schramm 2000). A typical product is AN125 from SNF Floerger. It hardly loses viscosity after 220 days of ageing at 100˚C with a calcium tolerance about four times as high as that of HPAM (Levitt and Pope 2008). Coreflood tests also proved it can be successfully used with seawater for temperatures as high as 90˚C (Bataweel 2011). But, for higher temperature over 105˚C, AMPS polymer will meet serious problems of degradation and precipitation (Vermolen et al. 2011; Gaillard et al. 2014). Therefore, the co-polymers or the ter-polymers with monomers of N-vinyl pyrrolidone (NVP) are prepared to provide tolerance to high temperature due to a neighboring effect between the AM and NVP units (Hsieh et al. 1992; Fernandez 2005). Polymers with AMPS and NVP (<25 mol%) can maintain viscosity over 60 days at 105˚C. At 120˚C, with a higher NVP concentration of 35~50%, the polymer keeps stable in seawater for at least one year (Vermolen et al. 2011; Gaillard et al. 2014). However, the cost of NVP polymer is relatively high. The reactivity of NVP is lower than AM during

the polymerization process, leading to drifts of composition and low molecular weight, which means more dosage and cost is required to achieve the target viscosity (Gaillard et al. 2010). In this study, the reservoir temperature is 194˚F (90˚C), so the AMPS polymer AN125 is selected in consideration of effectiveness and economy.

Simulation method is carried out to study polymer performance such as shear thinning, thermal thinning, retention, inaccessible pore volume and degradation in heterogeneous multilayered reservoir (Vela et al. 1976; Clifford and Sorbie 1985; Lee 2011). To realistically describe reservoir response to polymer, the simulation study must include all significant physicochemical phenomena in the polymer-reservoir system.

If large amounts of cool water, such as seawater with surface temperature, are injected into a hot reservoir, significant changes in temperature could be happen and calculations must take account of this (Brown et al. 1982; Sorbie et al. 1982). In a hot heterogeneous reservoir, the temperature distribution becomes uneven after cold water injected for several years. For such a reservoir, simulation results showed the final recovery factor for polymer with temperature-dependent degradation is between that of ideally stable polymer and polymer with non-temperature-dependent degradation (Sorbie and Clifford 1988). Besides the temperature influence on polymer, simulation study of an Indonesian oilfield showed the incremental oil recovery could also benefit from decrease in oil viscosity caused by injected geothermal hot water (Pederson and Sitorus 2001). The key is that the viscosity of oil will drop from 14cp to 2cp when temperature increases from 110°F to 300°F. For 20 year hot water injection, incremental recovery factor can be increased by over 7.5%, compared to cold waterflood at the same injection rate.

By 2013, 481 polymer flood projects were reported, and only 13.5% of them were discouraging (Saleh et al. 2014). In 2008, besides approximately 20 ongoing projects in China, there are one field project in India, one project in Argentina, and two in the US. Polymer flood contributed 22.3% of total production in Daqing Oilfield with an increase in ultimate oil recovery by 10%, because of its favorable conditions: Suitable reservoir heterogeneity (Dykstra-Parsons coefficient ranged from 0.4~0.7), low salinity and hardness (formation water TDS ranged from 3000 to 7000 mg/L) and low reservoir temperature (45˚C) (Dong et al. 2008). The upper temperature limit of polymer flood is commonly believed to be 70˚C. Almost all the polymer flood tests were carried out in reservoirs under 65˚C. For higher temperature condition, polymer flooding recovery performance is not very superior, especially when salinity is also high. A polymer flood field test in N.E.Hallsville Carane in America was carried out in 1965 with reservoir temperature of 109.4˚C, resulting in a 3.3% incremental recovery factor (Moore 1969). Another polymer flood was carried out in a thick reservoir of Shuanghe oilfield with reservoir temperature of 72˚C in 1994, resulting in a 10.4% incremental recovery factor, mainly thanks to the fine characterization of reservoir and use of high molecular weight polymer with thermal-oxidization stabilizers (He et al. 1998). Several pilot tests of polymer flood were carried out in Shengli Oilfield with reservoir temperature from 65˚C to 80˚C in different blocks (Gao 2014). Shengtuo block in Shengli Oilfield has the most harsh reservoir condition. The reservoir temperature is 80˚C, and the formation salinity is 21,000 mg/L. A comb polymer called KYPAM was selected, dissolved in produced water

with salinity of 12,400 mg/L. Polymer slug injected was 0.25PV, resulting in an incremental oil recovery of 4.655%.

1.3 History of Stratification Injection and In-Depth Profile Control

Polymer may break through very quickly due to existence of high permeability zone, resulting in poor improvement for sweep efficiency. Stratification injection, or separate layer injection, is a method to improve the sweep efficiency when cross flow does not occur between adjacent strata (Dong et al. 2008). According to theoretics and pilot application, the favorable conditions for this method include:

1. The permeability differential among oil zones is over 2.5.

2. The net pay with lower permeability should contain at least 30% of the total net pay.

3. At least one meter barrier between layers, and consistent lateral continuity between wells.

If good barrier does not exist, gel treatments or other types of profile control methods, which can divert injection fluid to un-swept areas (Nasr-El-Din et al. 1998), are considered to be valuable before implementation of a polymer flood (Sorbie and Seright 1992). A major drawback of near-wellbore gel treatments is that displacing fluid bypasses the gel and flows back to the high permeability zone, resulting in little effect on decrease on water cut and increase on incremental oil recovery (Al-Adasani and Bai 2010). In-depth

profile control began popular in the later 1990s when an interlayer heterogeneity conflict dominated in most of mature oilfields. Large volumes of treatment are used and much more effective in improving the seep efficiency. The typical in-depth profile control systems are colloid dispersion gel (CDG), particle gels, and a polymer-crosslinker-retarder weak gel system. Gel formed by PAM-based polymer and Polyethyleneimine (PEI) crosslinker has been proved to be stable in 2% KCl at 100 ˚C (Al-Muntasheri et al. 2007).

Recovery effects of polymer flood and in-depth profile control are compared in the aspect of polymer viscosity, oil viscosity, gel slug size, permeability contrast and vertical order of permeability (Okeke and Lane 2012; Seright et al. 2012). It is found that the in-depth profile control prefers the reservoir with high permeability contrasts, high thickness ratio and low oil permeability. But such method may not have as high oil recovery and monetary value as polymer flood.

1.4 Mechanisms of Polymer Flood

Polymer solution can increase the volumetric sweep efficiency in heterogeneous reservoirs, and some of the oil trapped in low permeability regions will be displaced (**Figure 1.1**). Thus the final oil recovery will be increased within economic limit. On the other hand, polymer solution can also increase fraction of oil in produced fluids with

relatively high mobile oil saturation in homogeneous reservoirs, which means more oil will be recovered with in same period, compared to waterflood with low viscosity.

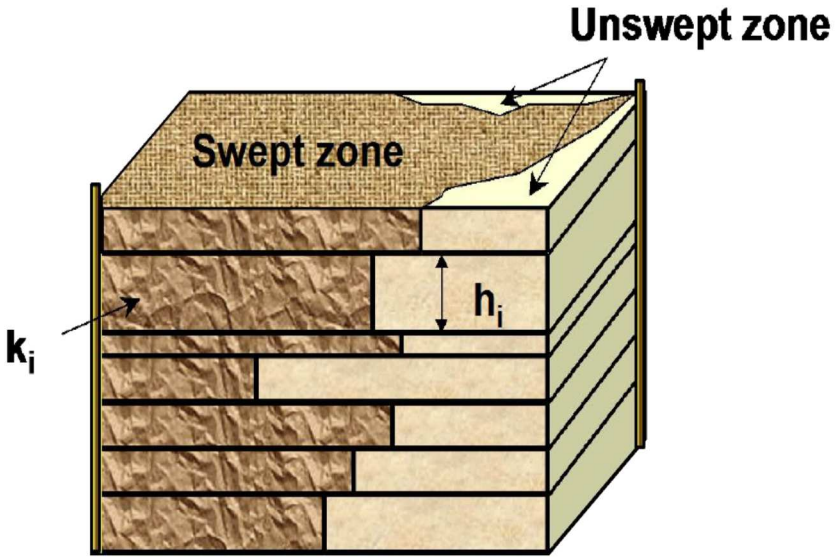

Figure 1.1: Sweep of displacing fluid in heterogeneous reservoir

2. A REVIEW OF CMG STARS SIMULATOR AND MODEL DESCRIPTION

2.1 General Description of the Simulator

CMG_STARS is a three-phase multi-component thermal and steam additive simulator. The version used for this study is 2013.13. It supports two-dimensional and three-dimensional configurations with grid systems of Cartesian, corner point, cylindrical and variable depth/variable thickness (STARS User's Guide). All blocks are treated in a fully implicit manner. The polymer models of STARS include Viscosity vs. Polymer Concentration, Viscosity vs. Shear Rate, Adsorption, Permeability Reduction, Inaccessible Pore Volume and Effect of Salinity on Viscosity. STARS can history match laboratory coreflood data with very good agreement (Goudarzi et al. 2013).

2.2 Mass Conservation Equations

A conservation equation is constructed for each component of a set of identifiable chemical components that completely describe all the fluids of interest.

The general equation is

Rate of change of accumulation = Net rate of inflow from adjacent regions + Net rate of addition from sources and sinks

The following are the separate terms for fluid flow.

The accumulation term for a flowing and adsorbed component i:

$$\frac{\partial}{\partial t}\left[V_f\left(\rho_w S_w w_i + \rho_o S_o x_i + \rho_g S_g y_i\right) + V_v\ Ad_i\right]$$

The flow term of flowing component I between two regions is

$$\rho_w v_w w_i + \rho_o v_o x_i + \rho_g v_g y_i + \phi\rho_w D_{wi}\Delta w_i + \phi\rho_g D_{gi}\Delta y_i + \phi\rho_o D_{oi}\Delta x_i$$

The volumetric flow rates are

$$v_j = T\left(\frac{k_{rj}}{\mu_j r_j}\right)\Delta\Phi_j \qquad j = w, o, g$$

a. T is the transmissibility.

b. Dji (j=w,o,g) are the component dispersibilities in the three phases and are again the product of geometric factors and component dispersion coefficients.

c. The potential at a grid node is $\Phi j = pj - \lambda jgh$.

The well source/sink term for flowing component i is:

$$\rho_w q_{wk} w_i + \rho_o q_{ok} x_i + \rho_g q_{gk} y_i$$

The reaction source/sink term for component i is:

$$V\sum_{k=1}^{n_r}\left(s'_{ki} - s_{ki}\right)\bullet r_k$$

The aquifer source/sink term for water component is:

$$\sum_{k=1}^{n_f}\rho_w\ qaq_{wk}$$

qaq_w is a volumetric water flow rate through a block face k to/from the adjacent aquifer.

The following are the separate terms for energy flow.

The accumulation term for energy is:

$$\frac{\partial}{\partial t}\left[V_f \left(\rho_w S_w U_w + \rho_o S_o U_o + \rho_g S_g U_g\right) + V_v c_s U_s + V_r U_r \right]$$

The flow term of energy between two regions is

$$\rho_w v_w H_w + \rho_o v_o H_o + \rho_g v_g H_g + K \Delta T$$

K is the thermal transmissibility at the interface between the two regions

The well source/sink term for energy is:

$$\rho_w q_{wk} H_w + \rho_o q_{ok} H_o + \rho_g q_{gk} H_g$$

The reaction source/sink term for energy is:

$$V \sum_{k=1}^{n_r} H_{rk} r_k$$

a. S'_{ki} is the product stoichiometric coefficient of component I in reaction k.

b. S_{ki} is the reactant stoichiometric coefficient of component I in reaction k.

c. H_{rk} is the enthalpy of reaction k.

d. r_k is the volumetric rate of reaction k, calculated from a model for reaction kinetics.

The heat loss source/sink term for energy is:

$$\sum_{k=1}^{n_r} HL_k + HL_v + HL_c$$

a. HL_k is the rate of heat transfer to the region of interest through block face number k, from the adjacent formation. The heat transfer rate and heat accumulated in the overburden are calculated using an analytical solution for an infinite overburden.

Heat flow back into the reservoir block may occur.

b. HL_v is the rate of heat transfer calculated from a convective model.

c. HLc represents a constant heat transfer model.

The aquifer source/sink term for the energy is:

$$\sum_{k=1}^{n_f} (HA_{CV} + HA_{CD})_k$$

a. HACV is a rate of heat transferred by convection to/from the adjacent aquifer.

b. HACD is a rate of heat transferred by conduction to/from the adjacent aquifer.

In summary, the (spatially discretized) conservation equation of flowing component I is:

$$\frac{\partial}{\partial t}\left[V_f\left(\rho_w S_w w_i + \rho_o S_o x_i + \rho_g S_g y_i\right) + V_v Ad_i\right]$$
$$= \sum_{k=1}^{n_f}\left[T_w \rho_w w_i \Delta\Phi_w + T_o \rho_o x_i \Delta\Phi_o + T_g \rho_g y_i \Delta\Phi_g\right] + V\sum_{k=1}^{n_r}\left(s'_{ki} - s_{ki}\right)r_k$$
$$+ \sum_{k=i}^{n_f}\left[\phi D_{wi} \rho_w \Delta w_i + \phi D_{oi} \rho_o \Delta x_i + \phi D_{gi} \rho_g \Delta y_i\right] + \delta_{iw}\sum_{k=1}^{n_f} \rho_w qaq_{wk}$$
$$+ \rho_w q_{wk} w_i + \rho_o q_{ok} x_i + \rho_g q_{gk} y_i \ [\text{well layer k}]$$

where n_f is the number of neighboring regions or grid block faces.

And the (spatially discretized) conservation equation of energy is

$$\frac{\partial}{\partial t}\left[V_f\left(\rho_w S_w U_w + \rho_o S_o U_o + \rho_g S_g U_g\right) + V_v c_s U_s + V_r U_r\right]$$
$$= \sum_{k=1}^{n_f}\left[T_w \rho_w H_w \Delta\Phi_w + T_o \rho_o H_o \Delta\Phi_o + T_g \rho_g H_g \Delta\Phi_g\right] + \sum_{k=1}^{n_f} K \Delta T$$
$$+ \rho_w q_{wk} H_w + \rho_o q_{ok} H_o + \rho_g q_{gk} H_g \text{ [well layer k]}$$
$$+ V \sum_{k=1}^{n_r} H_{rk} r_k + HL_o + HL_v + HL_c + \sum_{k=1}^{n_f} \left(HA_{CV} + HA_{CD}\right)_k$$

The phase transmissibilities T_j are

$$T_j = T\left(\frac{k_{rj}}{\mu_j r_j}\right) \qquad j = w, o, g$$

2.3 Boundary Condition

The boundary condition assumed is no convective, no dispersive, and no thermal flux through all boundaries.

2.4 Modeling of Polymer Properties

2.4.1 Polymer Solution Viscosity at Zero Shear Rate

The nonlinear mixing option partitions all the components into two groups: key components and those are not. The saturations (x_i) of these two groups sum to 1.

$$\Sigma_{i=S}\, x_i + \Sigma_{i\neq S}\, x_i = 1$$

To accomplish nonlinear mixing via alternate weighting factors, x_i is replaced with $f_i(x_i)$ for each i=S and with $N \cdot x_i$ for each i≠S, where N is a normalizing factor derived as follows.

$$\Sigma_{i=S} f_i(x_i) + N \cdot \Sigma_{i \neq S} x_i = 1$$
$$N = [\ 1 - \Sigma_{i=S} f_i(x_i)\ ] / [\ \Sigma_{i \neq S} x_i\ ]$$

Thus the nonlinear mixing rule for viscosity is calculated as:

$$\ln(\mu) = \Sigma_{i=S} f_i(x_i) \cdot \ln(\mu_i) + N \cdot \Sigma_{i \neq S} x_i \cdot \ln(\mu_i)$$

The function fi(xi) has three possible distinct ranges of xi values:

$$0 \leq x_i < x_{low}: \quad f_i(x_i) = x_i \cdot (f_1 / x_{low})$$
$$x_{low} \leq x_i \leq x_{high}: \quad f_i(x_i) \text{ from table look-up}$$
$$x_{high} < x_i \leq 1: \quad f_i(x_i) = f_{11} + (x_i - x_{high}) \cdot (1 - f_{11}) / (1 - x_{high})$$

2.4.2 Shear Thinning

A simple power law relation or a tabular input is available in STARS for modelling shear-rate-dependent viscosity relation.

The lab and modelling data from literature showed that the shear thinning effect is unobvious when divalent ions have the concentration as high as that in seawater (Kang et al. 2013). So the shear thinning effect is not modeled in this study.

2.4.3 Thermal Thinning

As temperature increases, the viscosity of polymer solution decreases. At higher temperature, the interaction among moieties becomes weaker, and the polymer chain tends to be more coiled. The solvation effect also becomes weaker, leading to a thinner water membrane around polymer molecular and smaller polymer bulk volume. Additionally, the viscosity of water also decreases (Al-Shammari et al. 2011). All these factors contribute to decreasing viscosity as the temperature increases.

Either a viscosity correlation contains two parameters or a tabular input is available for modelling temperature-dependent viscosity relation. The tabular input is used for this study. The parameters are obtained from lab experiments.

2.4.4 Polymer Adsorption and Resistance Factor

The retention of polymer has two mechanisms: mechanical entrapment and adsorption processing. Both of them depend on rock permeability. For sandstone, the permeability has a positive correlation to porosity. Lower permeability region means the pore there is smaller, which can entrap more polymer. And the surface area at that region is also bigger and can adsorb more polymer (Choi et al. 2014).

The Langmuir adsorption isotherm gives the adsorbed moles of component per unit pore volume as

$$\mathrm{ad} = \frac{(\mathrm{tad1} + \mathrm{tad2} * \mathrm{xnacl}) * \mathrm{ca}}{(1 + \mathrm{tad3} * \mathrm{ca})}$$

where xnacl is the salinity of the brine, and ca is the mole fraction of component. At high concentrations (large ca) the maximum adsorption is (tad1 + tad2 *xnacl)/tad3.

The maximum adsorption after flooding for a long time depends on the values of both key words ADMAXT (maximum adsorption) and ADRT (residual adsorption for a particular component) that specified. ADRT can take any value between zero and the ADMAXT value.

When ADRT equals zero (the default value), it models a completely reversible adsorption, i.e. when the concentration of the adsorbing component becomes less than that at which the maximum adsorption occurs, some of the adsorbed component gets desorbed and goes back into the aqueous phase. When the concentration of the adsorbed component becomes zero, then complete desorption occurs. On the other hand, if ADRT equals the ADMAXT value, then the adsorption is completely irreversible, i.e. once adsorbed the component does not get desorbed into the aqueous phase even when the component's concentration in the aqueous phase reduces. Any value of ADRT that lies between 0 and ADMAXT models a partially reversible adsorption.

Adsorption or mechanical entrapment can cause blockage which amounts to a reduction in the effective permeability. This is accounted for by the permeability reduction factors

RKW = 1 + (RRF-1) * AD(C,T)/ADMAXT

RKO = 1 + (RRF-1) * AD(C,T)/ADMAXT

RKG = 1 + (RRF-1) * AD(C,T)/ADMAXT

which affects the permeabilities AKW(I), AKO(I), AKG(I) as

AKW(I) = AK(I) * krw/RKW(I)

where AK(I) is standard block permeability.

Considering the temperature effect on polymer adsorption is very small, compared with other effect such as thermal thinning and degradation, the modeling of polymer adsorption in this study is simplified. The parameters used are same as those in CMG sample case for sandstone, and there's no difference for layers with various permeability. The retention of polymer is irreversible.

2.4.5 Degradation

Degradation is assumed to be a first-order chemical reaction, and modeled with the Arrhenius Equation. The reactants is polymer, and the resultant is water. The reaction rate depends on activation energy and reaction frequency factor.

2.5 Relative Permeability Model

Multiphase relative permeabilities are modeled based on Corey-type functions.

Krw = Krwiro * ((Sw - Swcrit)/(1.0 - Swcrit - Soirw))^Nw

Krow= Krocw * ((So - Sorw)/(1.0 - Swcon - Sorw))^Now

Krog= Krogcg * ((Sl - Sorg)/(1.0 - Sgcon - Sorg))^Nog

Krg = Krgcl * ((Sg - Sgcrit)/(1.0 - Sgcrit - Soirg))^Ng

2.6 Gel Modeling

2.6.1 Gelation Reaction

Similar as polymer degradation, the modeling of gelation reaction is also based on Arrhenius Equation. The reactants are polymer and crosslinker, and the resultant is gel. The reaction rate depends on activation energy and reaction frequency factor.

2.6.2 Gel Retention and Resistance Factor

The same model as polymer retention is used for gel retention. Gel retains on rock surface and slows down water phase flow velocity. The degree of water velocity slowing down is determined by the resistance factor of gel. A Langmuir-type isotherm is conducted and the process is irreversible.

2.7 Thermal Parameters

Yoshioka and Dawkrajai (Dawkrajai et al. 2006; Yoshioka et al. 2007) simulated the temperature change when fluids flowed to the wellbore during the depletion recovery and water coning. The temperature change was determined by the elevational geothermal temperature change and Joule-Thomson effect. The maximum change of temperature was around 2F. The value of heat capacity and thermal conductivity in the paper is similar to that in Sorbie's polymer flood study (Clifford and Sorbie 1985; Sorbie and Clifford 1988), which is the default value given by CMG.

2.8 Basic Assumption for Modeling

Very low fluid compressibility and thermal expansion are set to minimize the change of fluid volume due to temperature variation, making the comparison of recovery effect easy.

There is no heat transfer at boundary. The model with heat transfer at boundary has been tested and found this effect is negligible. Another study carried out by Xingru Wu (Wu et al. 2013) modeled the thermal retardation for water injection. It mentioned that heat conduction from overburden and underburden is neglected since it is a second order effect. The heat conduction from the overburden and underburden can be approximated by an error function using a concept of thermal penetration depth. It's a slow process compared with the conduction heat transfer. Thus the heat transfer is not modeled for this study. However, this effect could be significant for extremely high temperature contrast condition such as steam flood.

Retention and resistance factor is constant for all the rocks. Although for sandstone, retention of chemicals depends on the pore size and structure of rocks, the difference could be neglected for this study.

2.9 Detail of Model in this Study

A cuboid reservoir model is built with parameters obtained from literatures about highly stratified Brent sands in the North Sea (Sorbie et al. 1982; Clifford and Sorbie 1985; Sorbie and Clifford 1988). The well pattern in this study is different from that in literatures, which was line pattern. Although the line pattern and inverted 9-spot pattern can make the

incremental recovery a little bit higher than the 5-spot pattern, the line pattern has a poorer connectivity, and the inverted 9-spot pattern has worse injection capacity (Dong et al. 2008). Therefore, the 5-spot pattern with one injector in the center and four producers in the corners appears attractive for polymer flood, which is used for this study (**Figure 2.1**).

To model a stratified reservoir with high permeability contrast, 5 layers have different permeability. From bottom to top, layer 1 and 5 have permeability of 12 md and thickness of 40ft. Layer 2 and 4 have permeability of 60 md and thickness of 30 ft. And layer 3 in the center has permeability of 600 md and thickness of 37 ft (**Figure 2.2**). The porosity of each layer has a correlation to permeability, ranging from 0.16 to 0.24. This correlation is generated from the sandstone model used in North Sea. The relative permeability curves are shown in **Figure 2.3**. Other critical parameters for this model are demonstrated in **Table 1**.

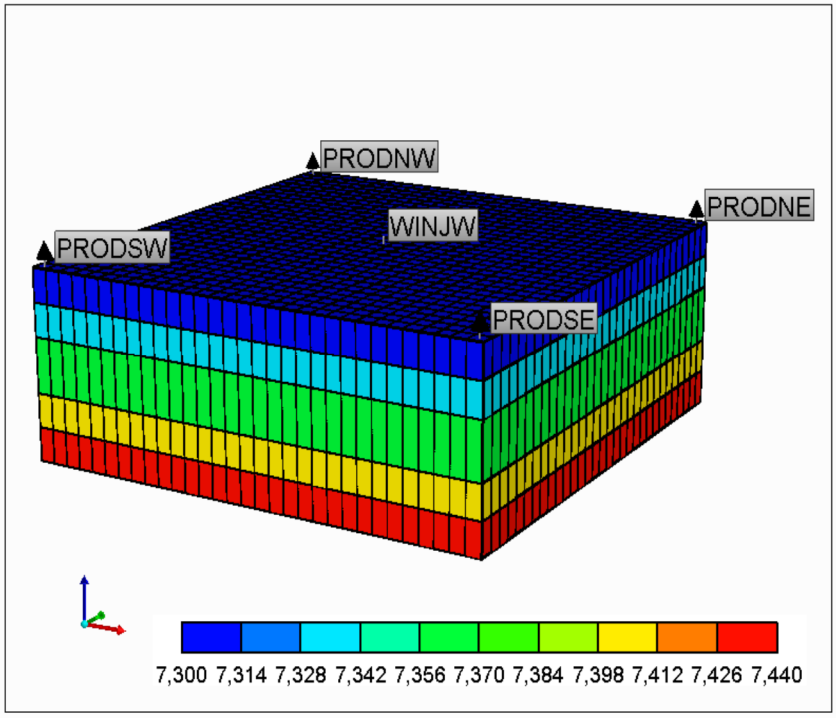

Figure 2.1: 5-Layer 5-Spot Synthetic Reservoir Model

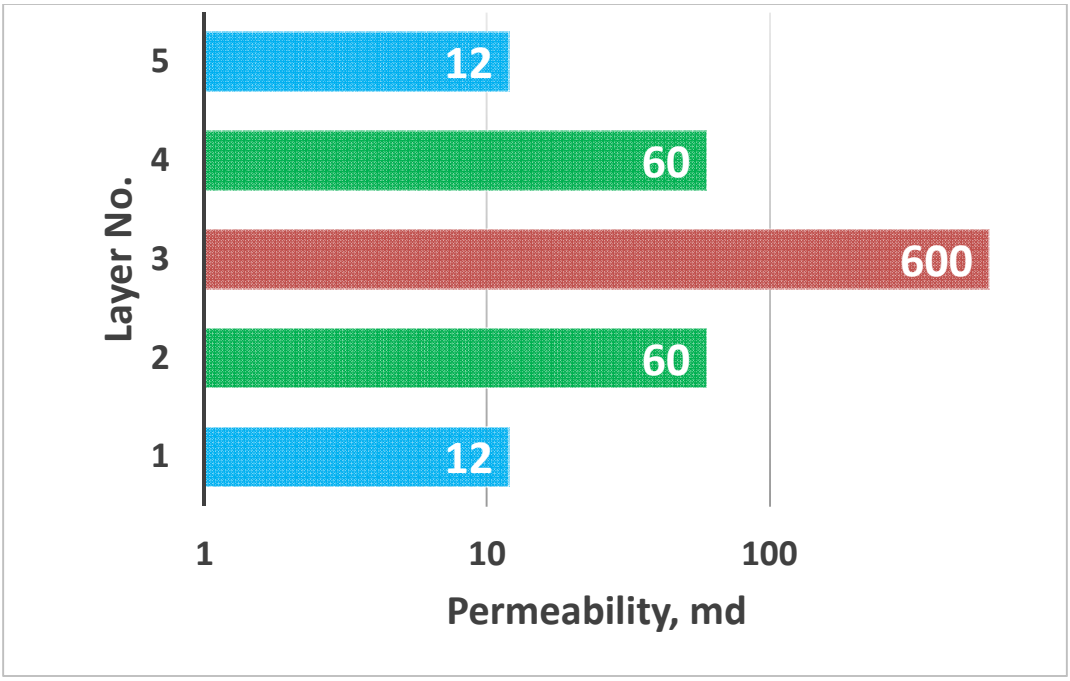

Figure 2.2: Permeability of each layer.

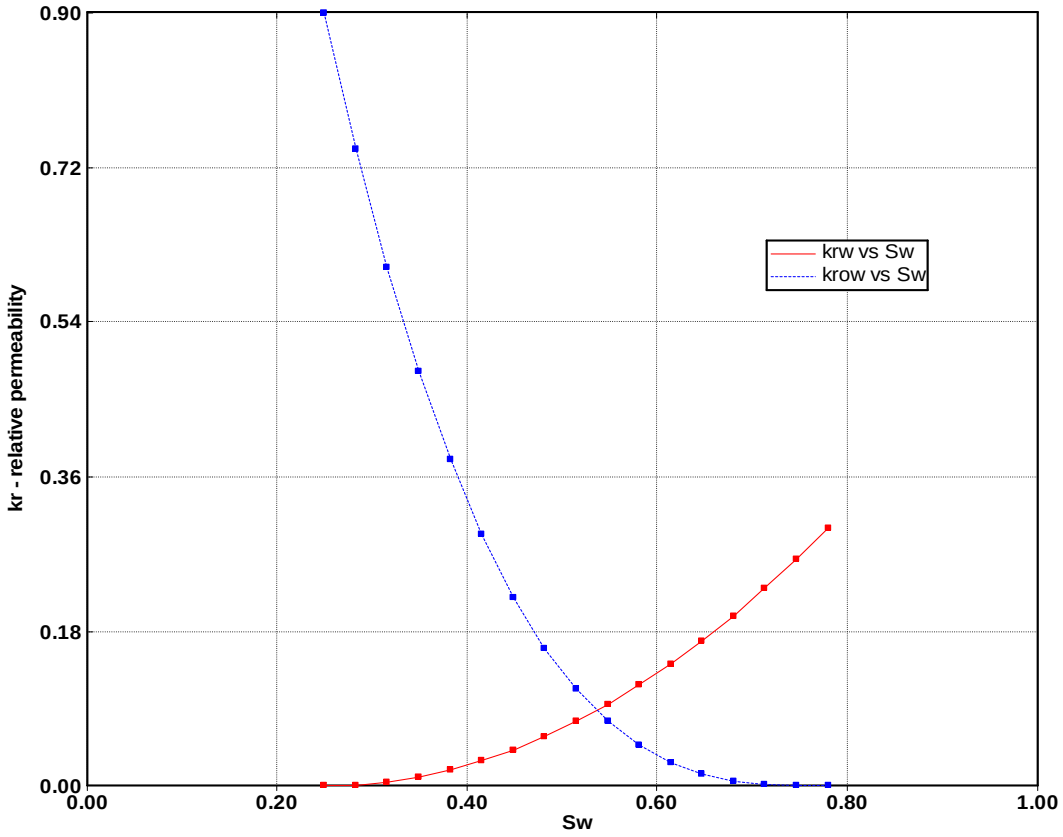

Figure 2.3: Relative permeability curves used for this study.

Table 2-1: SUMMARY OF RESERVOIR MODEL INPUT PARAMETERS	
Length, L ft	930
Width, W ft	930
Height, H ft	177
Number of grids in x, y, z	31 x 31 x 5

Table 2-2 Continued	
Cell dimensions in x direction, ft	30
Cell dimension in y direction, ft	30
Cell dimension in z direction, ft	40, 30, 37, 30, 40
Components simulated	Water, oil, polymer, gel, xlinker
Initial Reservoir Pressure, psi	3700
Initial Reservoir Temperature, °F	194
Porosity	0.16, 0.19, 0.24, 0.19, 0.16
Initial Water Saturation	0.25
Relative Permeability Curve Type	Water wet
Residual water saturation, fraction	0.25
Residual oil saturation, fraction	0.22
Endpoint relative permeability of water	0.3
Endpoint relative permeability of oil	0.9
Relative permeability exponent of water	2
Relative permeability exponent of oil	3
Heat capacity of rock, Btu/ft3-°F	35
Thermal conductivity of rock, Btu/ft-day-°F	44
Thermal conductivity of water, Btu/ft-day-°F	8.6
Thermal conductivity of oil, Btu/ft-day-°F	1.8
Injection Rate, PV/year	0.11

3. SHEAR THINNING AND THERMAL THINNING STUDY

3.1 Background

Polymer solution is a non-Newtonian fluid. Its viscosity is dependent on shear rate. Additionally, temperature also affects the viscosity. The reason for the above phenomena is that the macroscopic viscosity depends on the microscopic shape of molecular chain, which could be affected by shear rate and temperature.

3.2 Materials and Equipment

Co-polymer acrylamide and 2-acrylamido 2-methyl propane sulfonate (AMPS), which is called AN-125, were used as received from SNF Floergre (Cedex, France) in solid form. The molecular weight is $6x10^6$, and the degree of hydrolysis is 20-30%.

The water used in all experiment was prepared from a water system with resistivity greater than 18 MΩ-cm at 25˚C. Sodium chloride, magnesium chloride, calcium chloride, sodium bicarbonate, sodium carbonate and sodium sulfate used to prepare seawater were an analytical grade.

Grace Instrument M5600 HPHT Rhometer was used for measuring viscosity. The rheometer uses a bob-and-cup arrangement for rheological property determination. The liquid is placed inside an annulus between the two cylinders (bob and cup), where the cup (outer cylinder) is rotated at a set speed that determines the shear rate. The liquid between

the two cylinders exerts a drag force (torque) on the bob (inner cylinder), which is measured and converted to a shear stress.

The M5600's unique frictionless bob shaft construction and advanced sensor design enables the measuring of small changes in shear stress instantly by non-mechanically transmitting a zero friction rotational torque signal from the pressure containment area. The outer cylinder (sample cup) is driven by a stepper motor at speeds from 0.0001 – 1,100 rpm. The thermocouple probe measures the sample temperature at the tip of the bob shaft. All electronics and other sensitive components are protected from the influences of both the sample fluid and its vapor. (Operation Manual of M5600).

3.3 Experimental Procedure

Synthetic seawater was used to prepare polymer solutions using compositions shown in **Table 3-1**.

Table 3-1: SEAWATER COMPOSITION

Ions	Concentration, mg/L
Na^{+}	16,877
Ca^{2+}	664
Mg^{2+}	2,279
HCO^{3-}	193
Cl^{-}	31,107

Table 3-2 Continued	
$SO4^{2-}$	3,560
TDS	54,680

Polymer powder were weighted and mixed with seawater by a stirrer for 90 minutes. The concentration of polymer solutions was 1000, 2000, 3000, 4000 and 5000 ppm.

Rheology and viscosity measurements of all polymer/seawater systems were conducted at 300 psi. The viscosity of polymer solutions with various concentrations as a function of shear rate was measured over a range of 0.1 to 1000 s^{-1}, which included shear rates 0.1 – 10 s^{-1} encountered in chemical flooding (Nasr-El-Din et al. 1991). The viscosity was measured by increasing the shear rate. Shear rate changed when temperature kept stable at 194°F.

The viscosity of polymer solutions with various concentrations as a function of temperature was measured over a range of 78°F to 194°F at the shear rate of 100 s^{-1}.

3.4 Lab Results and Discussion

3.4.1 Shear Thinning Effect

The rheology curves of polymer/seawater solution with different concentration are showed in **Figure 3.1**.

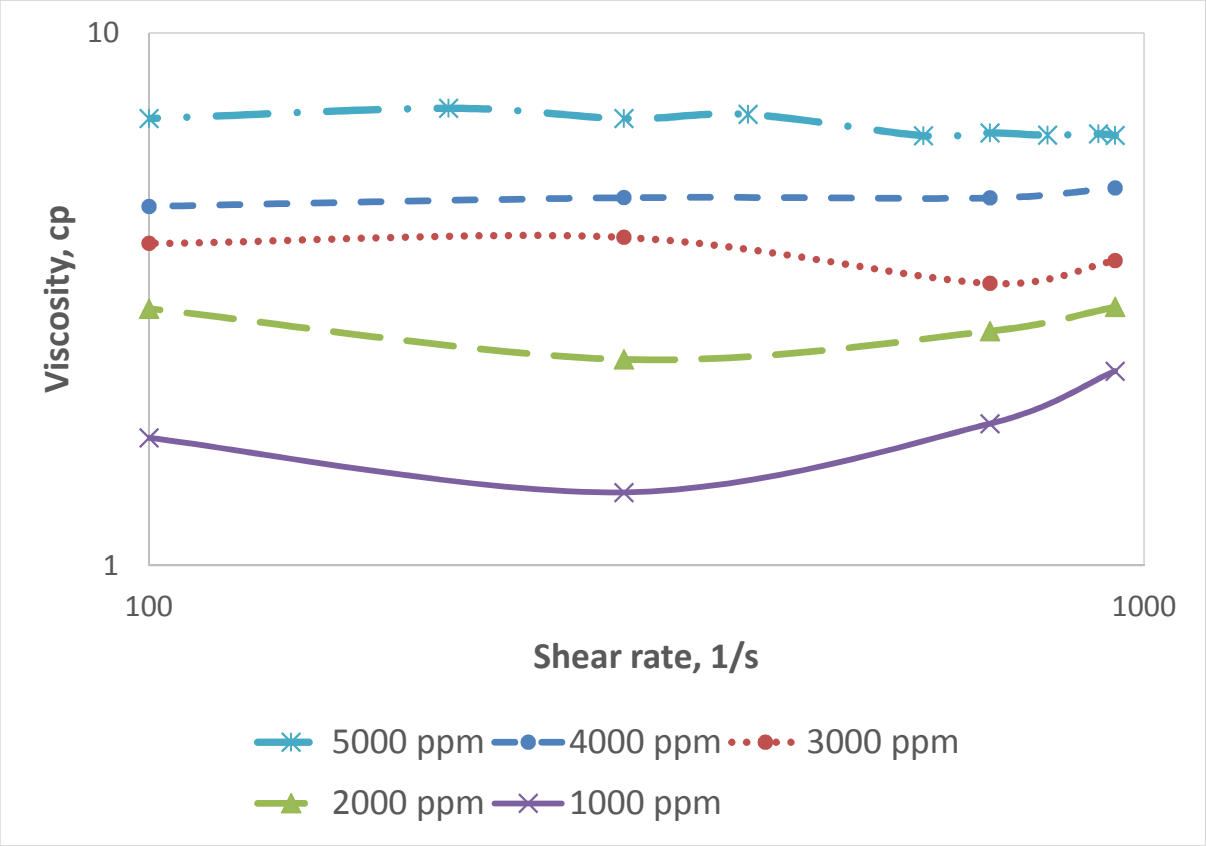

Figure 3.1: Viscosity vs shear rate for different concentration. The viscosity kept constant from 100 s^{-1} to 1000 s^{-1}.

Due to the limitation of the measurement range of this rheometer, only data ranging from 100~1000 s^{-1} is accurate for polymer solution. It is clear that the viscosity nearly does not change with shear rate for all solutions. The reason is that the both temperature and salinity are high. At such a condition, the interaction among moieties becomes weaker, and the polymer chain tends to be more coiled. The solvation effect also becomes weaker, leading to a thinner water membrane around polymer molecular and smaller polymer bulk volume. Additionally, the viscosity of water also decreases (Al-Shammari et al. 2011). All

these factors contribute to decreasing viscosity as the temperature increases. This results is in accordance with that in published paper (**Figure 3.2**).

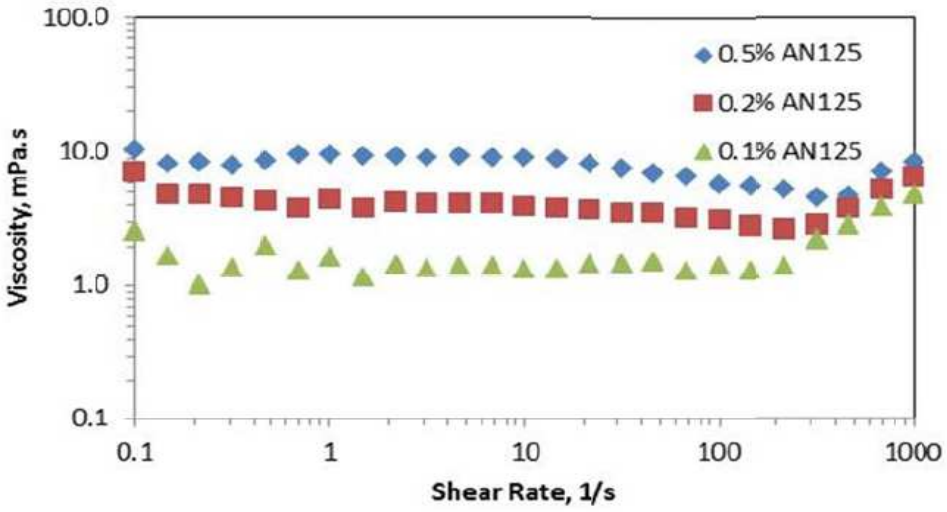

Figure 3.2: Rheology curves for different concentration tested by MCR 301 Rheometer. It also elucidates the viscosity of polymer/seawater solution at high temperature does not change too much when shear rates changed (Han et al. 2012).

3.4.2 Thermal Thinning Effect

The viscosity of 5000 ppm polymer/seawater solution were tested at $100s^{-1}$ with temperature increasing from 78°F to 194°F, shown in **Figure 3.3**. For polyacrylamides, the viscosity as a function of temperature scales roughly with the viscosity of water. Upon cooling down, the polymer solution viscosity will increase again, following a similar, but slightly lower curve (Vermolen et al. 2011).

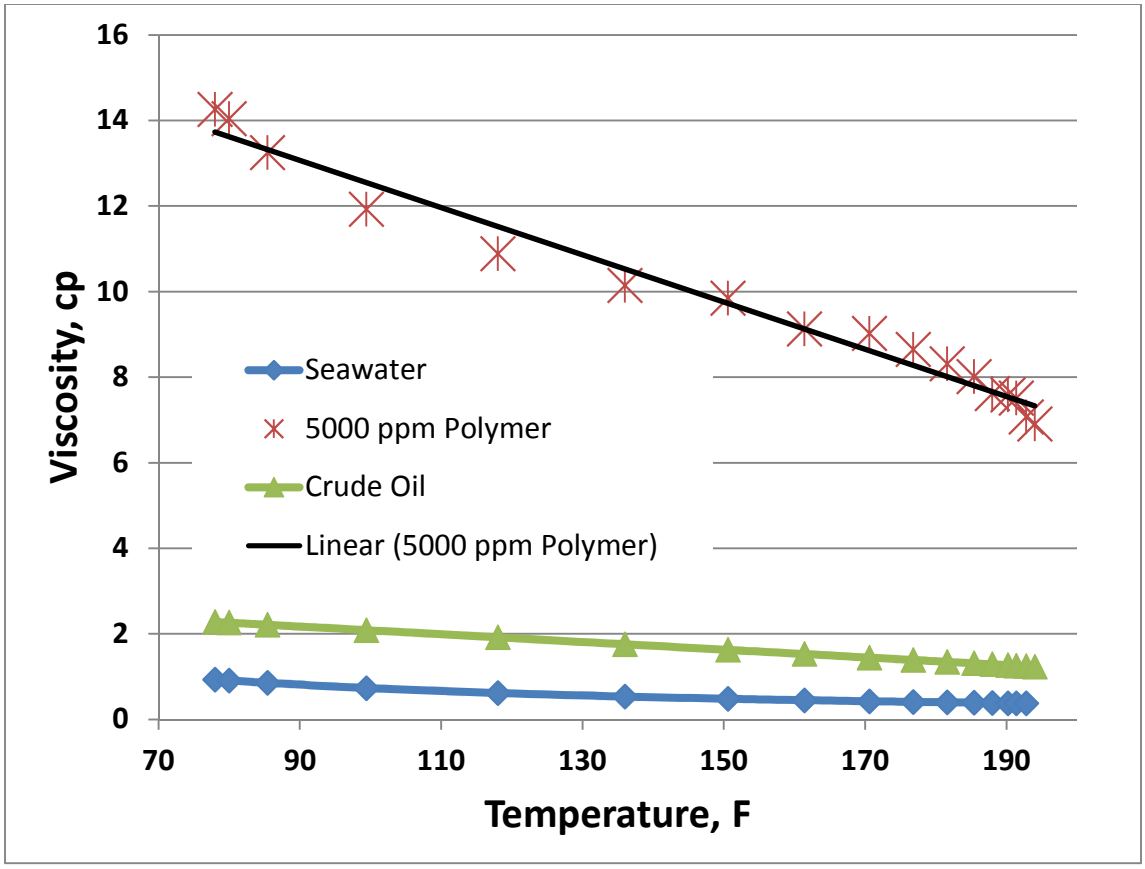

Figure 3.3: Viscosity vs temperature for crude oil, seawater and 5000 ppm polymer/seawater solution. The viscosity of crude oil, seawater and polymer solution decrease with temperature increase.

Similar properties are also found for other thermal-resistance polymers (**Figure 3.4**).

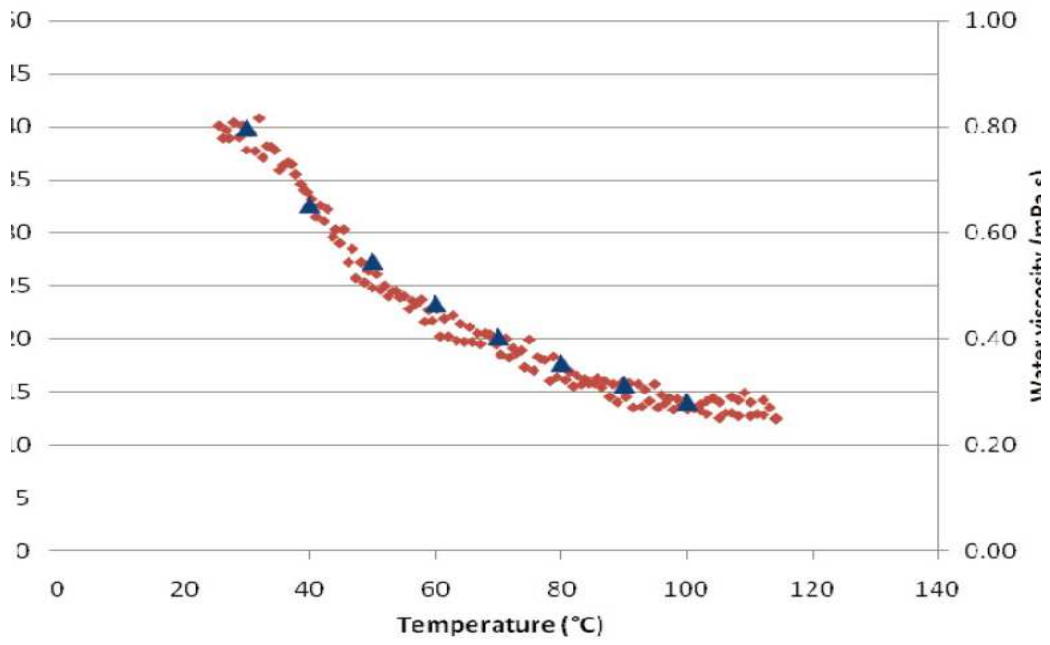

Figure 3.4: Viscosity of a 6000 ppm n-VP Polymer 3 solution in 200 g/l NaCl brine as a function of temperature (red dots), compared to the water viscosity (blue triangles).(Vermolen et al. 2011)

3.5 Simulation Input Description

A tabular input which indicates the relation between viscosity of fluids and temperature is used to model the thermal thinning effect. The input parameters are obtained from lab experiments and literatures.

3.6 Simulation Studies of Thermal Thinning in Homogenous Temperature Condition

15 cases in total were run to study the recovery performance of polymer flood in various even temperature condition. 5 temperature conditions were tested, including 78°F,

100°F, 120°F, 160°F and 194°F. To achieve an even temperature condition, the injection temperature was same as the reservoir temperature. Base cases of waterflood were simulated as benchmarks. For polymer flood cases, a 0.33 PV of seawater pre-flush slug was injected firstly, following by a 0.53 PV polymer seawater solution slug. The concentration of polymer used were 3000 ppm and 5000 ppm for each temperature condition. After polymer flood slug, a post-flush of seawater continued for 0.16 PV. **Figure 3.5** shows the injection scheme.

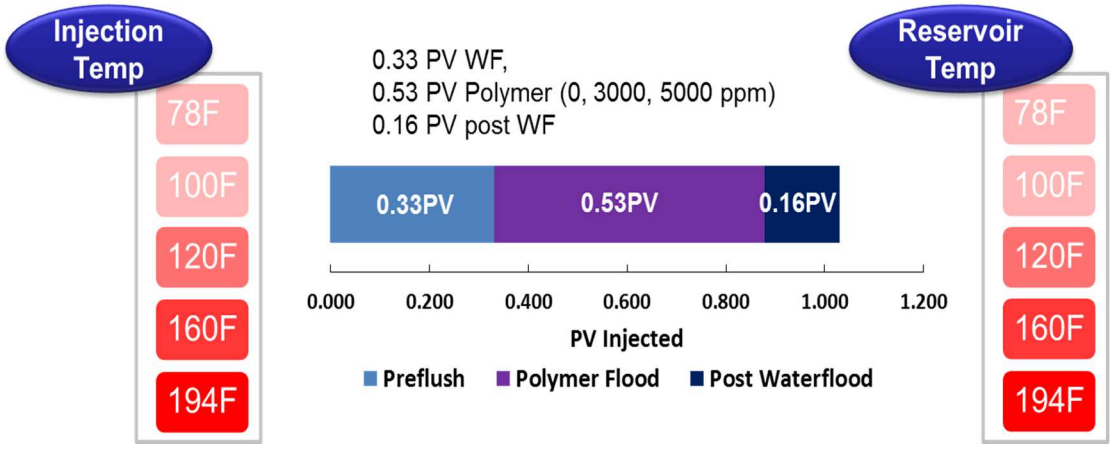

Figure 3.5: Injection scheme of homogeneous temperature cases.

Recovery effect is showed as recovery factors for waterflood and incremental recovery factors for polymer flood in **Figure 3.6**. For waterflood, the oil recovery factors are around 38% for all the cases. This is because the viscosity of both oil and seawater decreases with temperature increase. The offset keeps the mobility ratio of displacing phase and displaced phase stay akin. For polymer flood, the recovery factors for cases with same concentration are similar, due to the offset of mobility increase in both polymer

solution and crude oil. For 3000 ppm cases the incremental recovery factors are around 13%, while for 5000 ppm cases the incremental recovery factors are around 16%. Besides, it clearly shows that flood process with higher polymer concentration obtains higher final oil recovery factor.

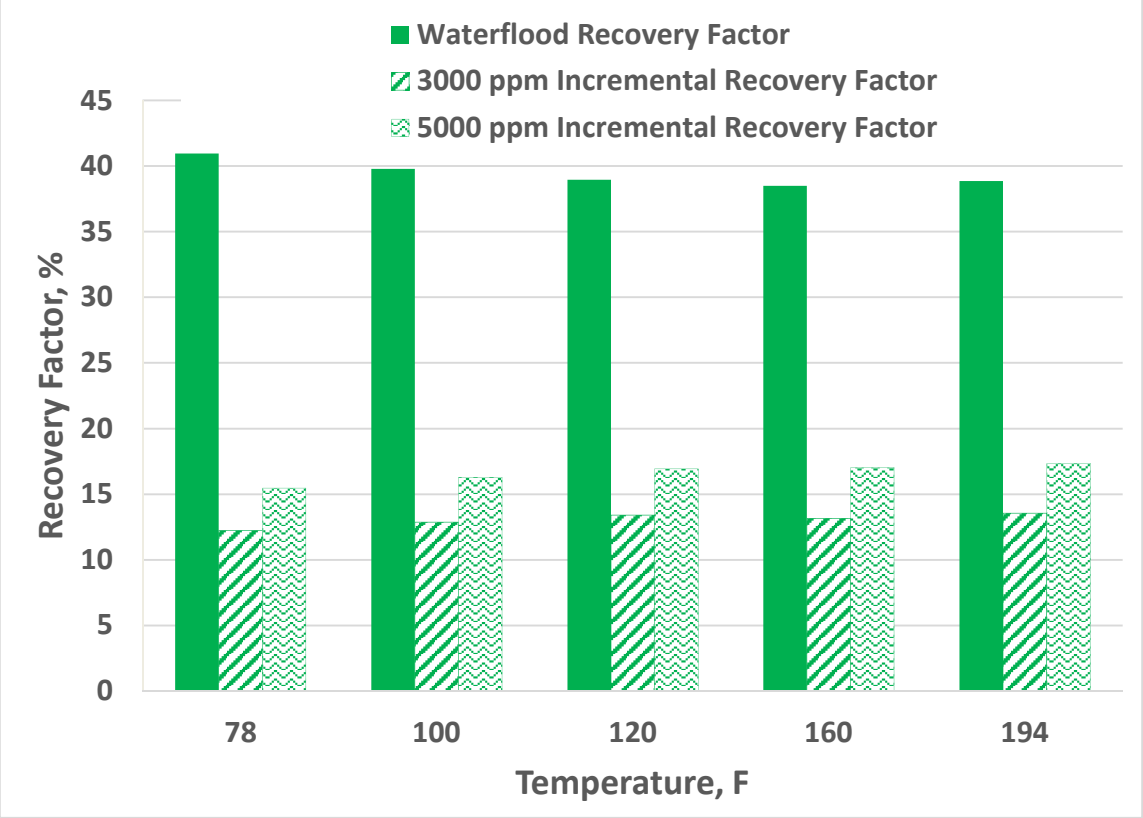

Figure 3.6: Waterflood recovery factor and polymer flood incremental recovery factor at even temperature conditions.

3.7 Simulation Studies of Thermal Thinning in Heterogeneous Temperature Condition

To study the recovery performance of polymer flood in uneven temperature condition caused by cool water injection, 6 cases were run. 3 cases with different polymer flood timing were carried out in an even temperature condition to study influence of timing of polymer injection (**Figure 3.7**). The injection of polymer was after the pre-flush slugs of 0.23, 0.34 and 0.45 PV, respectively for design 1, 2, and 3. The polymer slugs were 0.56 PV for all the designs. Post waterflood followed was 0.76, 0.65 and 0.54 PV, respectively. The total injection volume of the whole process is same for the three designs. The reservoir temperature is set to be 78°F, same as the injection temperature. Thus the temperature will not change.

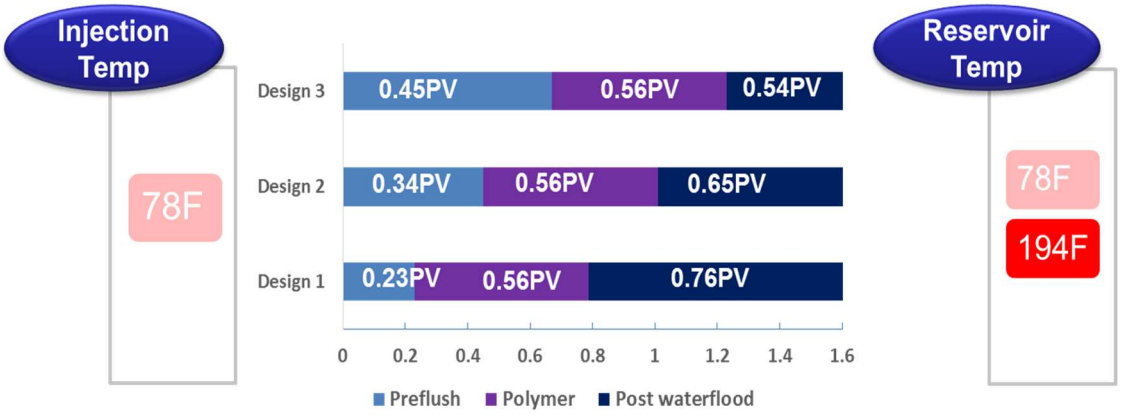

Figure 3.7: Injection scheme of heterogeneous temperature cases.

Another 3 cases were carried out to study the cool effect. Compared to the previous 3 cases in even temperature condition, these 3 cases had the same injection schemes, and

the only difference was the reservoir temperature. For the latter cases, the initial reservoir temperature was 194°F, and it was cooled down by injected seawater unevenly.

Recovery factors for even temperature condition are showed in the left of **Figure 3.9**. They are around 55% and no obviously different. It means the polymer injection timing hardly affects the final recovery factors in even temperature condition. In other words, for the same fraction of polymer slug in the total injection process, different oil saturation and distribution at the timing of polymer injection does not affect final recovery factor.

For cases with uneven temperature condition, the simulation results of cross sections indicate that temperature in high permeability layer is lower than that in the low permeability layers, because more water flushes the high permeability layer (**Figure 3.8**). And temperature in near well regions is lower than that in deep reservoir, due to longer sweeping time in near well regions. Additionally, with a larger pre-flush slug, more blocks are cooled to lower temperature.

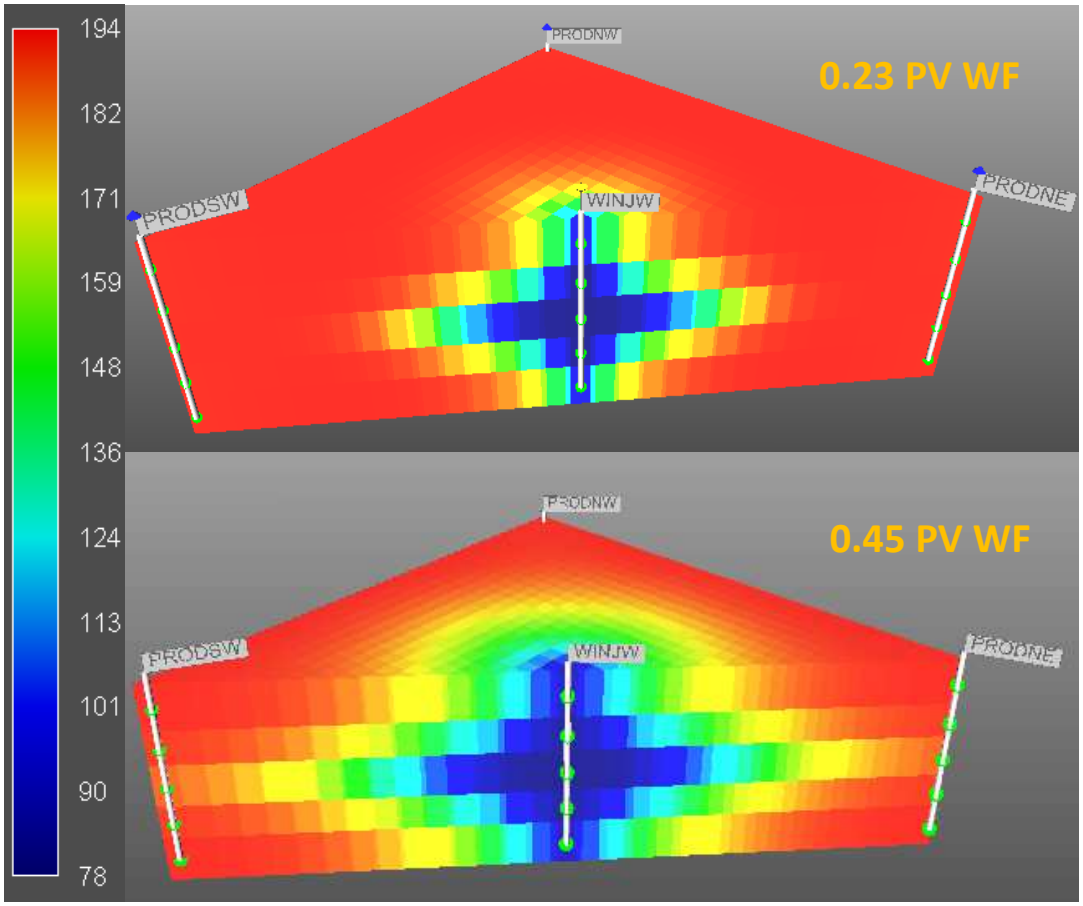

Figure 3.8: Temperature profiles for design 1 & 3 at the end of waterflood

The recovery factors of polymer flood in uneven temperature condition are shown in the right of **Figure 3.9**, which are also around 55%. It demonstrates that temperature difference does not affect the final recovery factor, also because decline trend of viscosity

is similar for both polymer solution and crude oil, no matter that the viscosity of polymer solution in low temperature region is double of that in high temperature region.

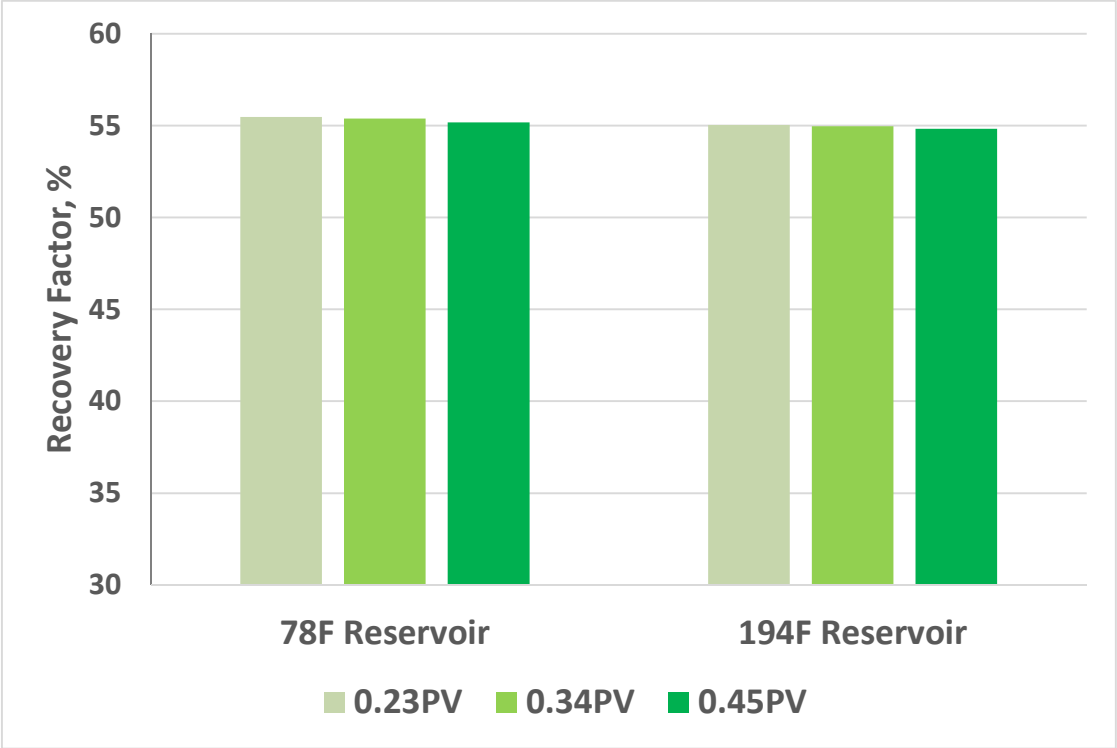

Figure 3.9: Recovery factors for polymer injection at different time.

3.8 Summary

Higher polymer concentration led to higher oil recovery. More polymer dissolved in the seawater will increase the water phase viscosity, thus deceases its mobility.

In reservoirs with high temperature, seawater flood before polymer injection cooled the reservoir unevenly.

Temperature difference caused by seawater flush does not obviously affect the final oil recovery factor, although lower temperature can largely increase viscosity of polymer solution.

4. THERMAL DEGRADATION STUDY

4.1 Background

Synthetic polymer degrades with high temperature and high oxygen concentration condition, which is the main reason for failure of polymer flood in high temperature reservoir. In this section the degradation behavior for AN125 is summarized from literature, and modeling parameters are generated. Then the effect of thermal degradation to polymer flood performance is studied by simulation method.

4.2 Simulation Input Description

Viscosity of AN125 solution with concentration of 1850 ppm decreases from 12 cp to 6 cp within 48 days at 221°F, which is the half-life of AN125 at this temperature (**Figure 4.1**). At 248°F, the viscosity of AN125 decrease to 50% of the initial within 15 days (**Figure 4.2**). Based on the two half-lives at two different temperature, the activation energy and reaction frequency factor of degradation reaction is calculated, based on the Arrhenius Equation.

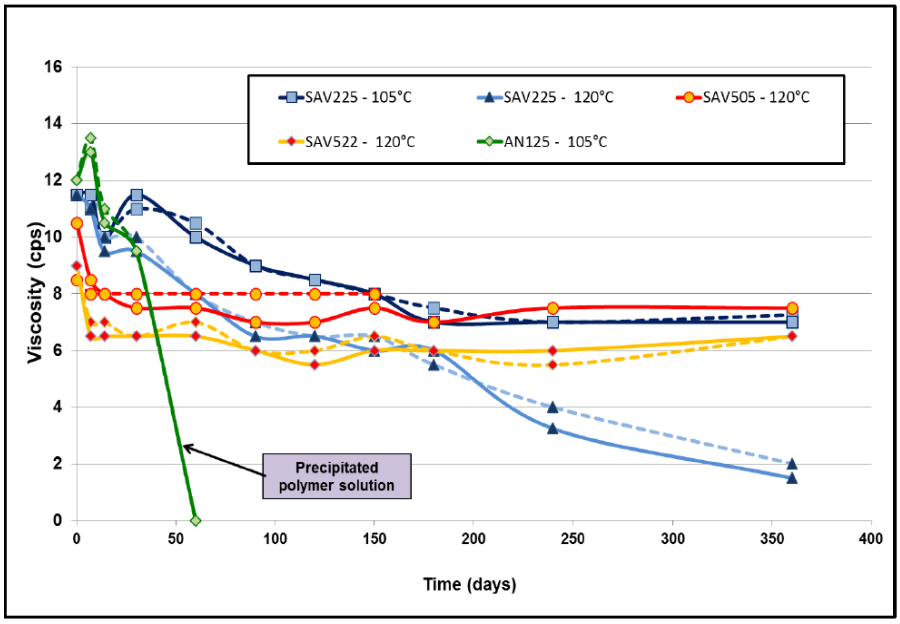

Figure 4.1: AN125 solution degradation curve at 221°F (Gaillard et al. 2014). The precipitation of polymer is considered as degradation in modelling.

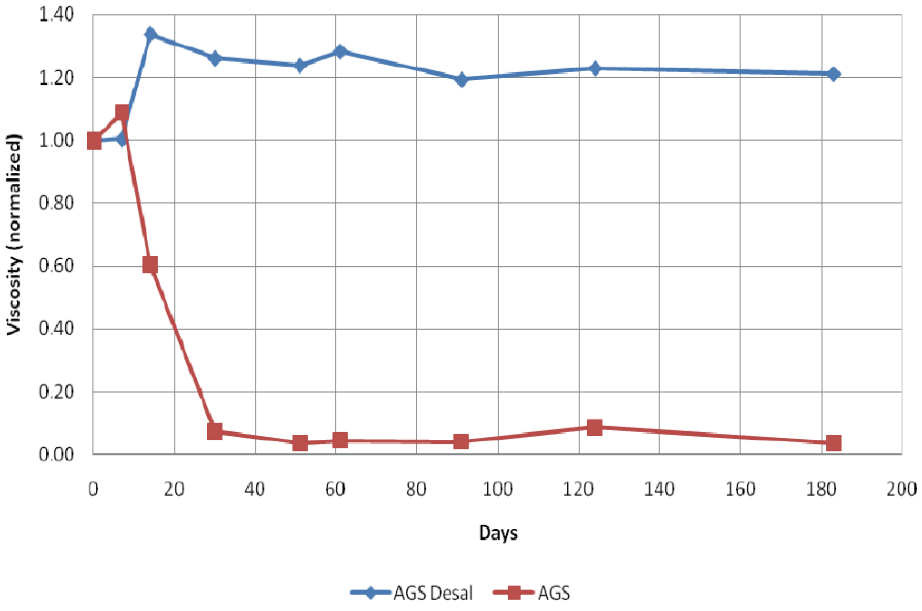

Figure 4.2: AN125 solution degradation curve at 248°F (Vermolen et al. 2011).

4.3 Simulation Studies of Temperature Influence

The modeling of polymer degradation behavior is verified through simulation of static processes. 4000 ppm polymer flood was injected to a core at very high rate and stopped. Then both injection and production were shut in for 500 days. This process was carried out at different temperature. Simulation result shows that the half-life at 221°F (**Figure 4.3**) and 248°F (**Figure 4.4**) are exactly the same as that indicated in literatures.

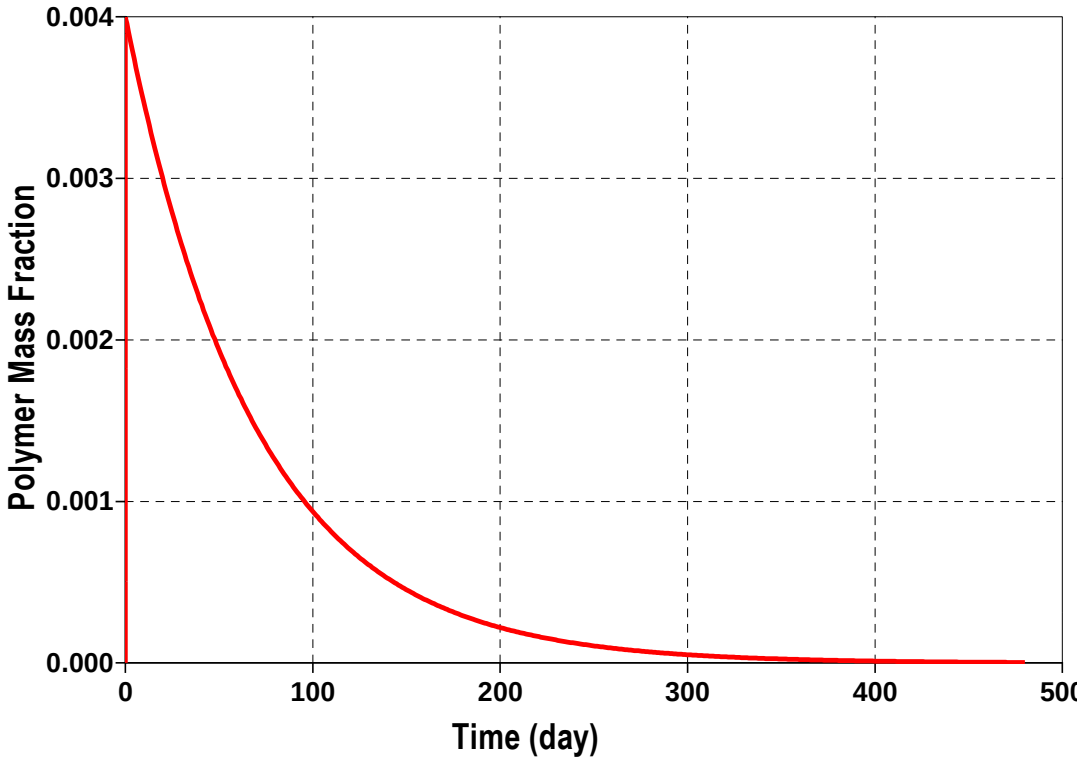

Figure 4.3: Polymer mass fraction declined due to degradation at 221°F.

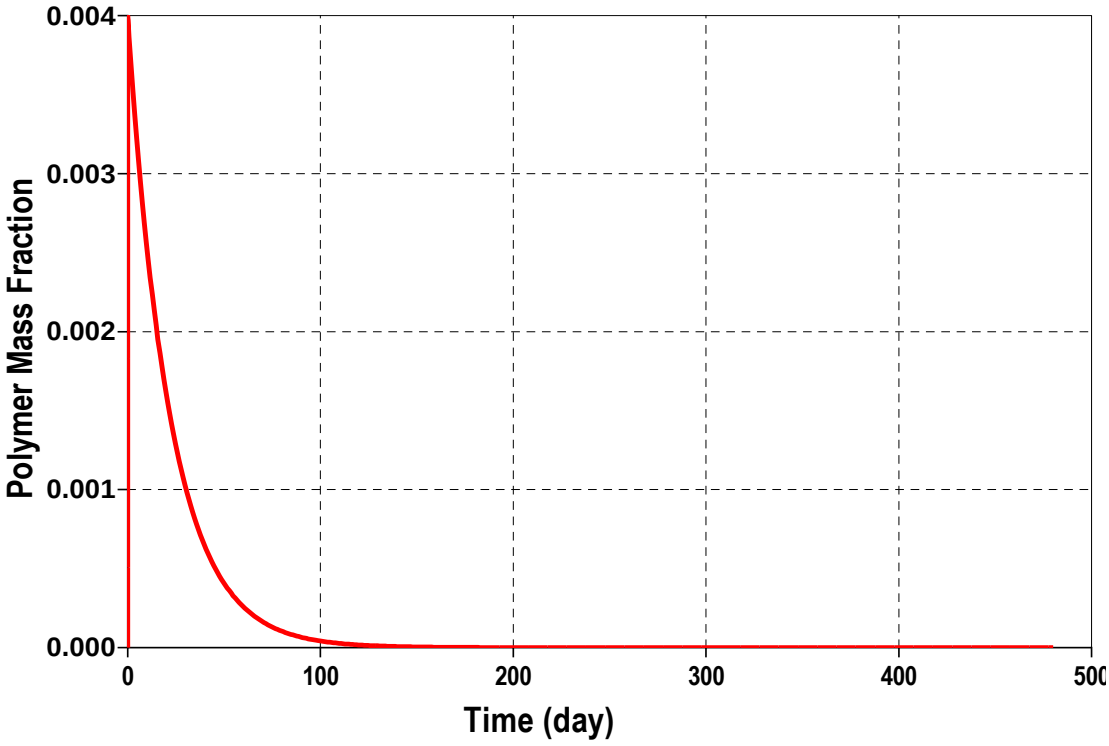

Figure 4.4: Polymer mass fraction declined due to degradation at 248°F.

The half-lives of polymer degradation at other temperature was also calculated (**Figure 4.5**). At 194°F, the half-life is 94 days, while at 78°F, it is 19,317 days. It means at lower temperature as 78°F, polymer solution does not significant lose viscosity through the whole flood process.

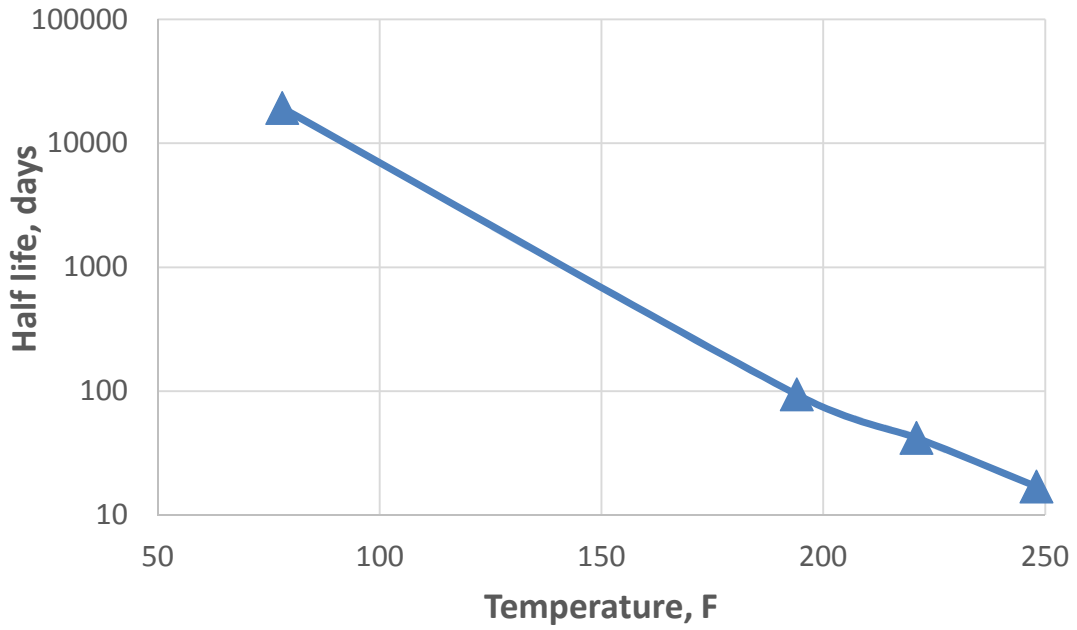

Figure 4.5: Simulation result showing that half-life of polymer declines with temperature increase.

A total of 4 polymer flood cases were run to study how degradation of polymer affects the final oil recovery factors, including 2 injection temperature of 78°F and 194°F, and 2 polymer concentration of 3000 ppm and 5000 ppm. All reservoir temperature is 194°F. The simulation results for these cases with degradation are compared to the cases with non-degradation.

The loss of final recovery factors with in varying degrees are observed (**Figure 4.6**). The reduction of recovery factor equals to recovery factor of non-degradation case minus recovery factor of degradation case. For same polymer concentration, higher injection temperature of 194°F makes bigger amount of polymer to degrade, leading to more reduction in recovery factor, compared to lower injection temperature of 78°F.

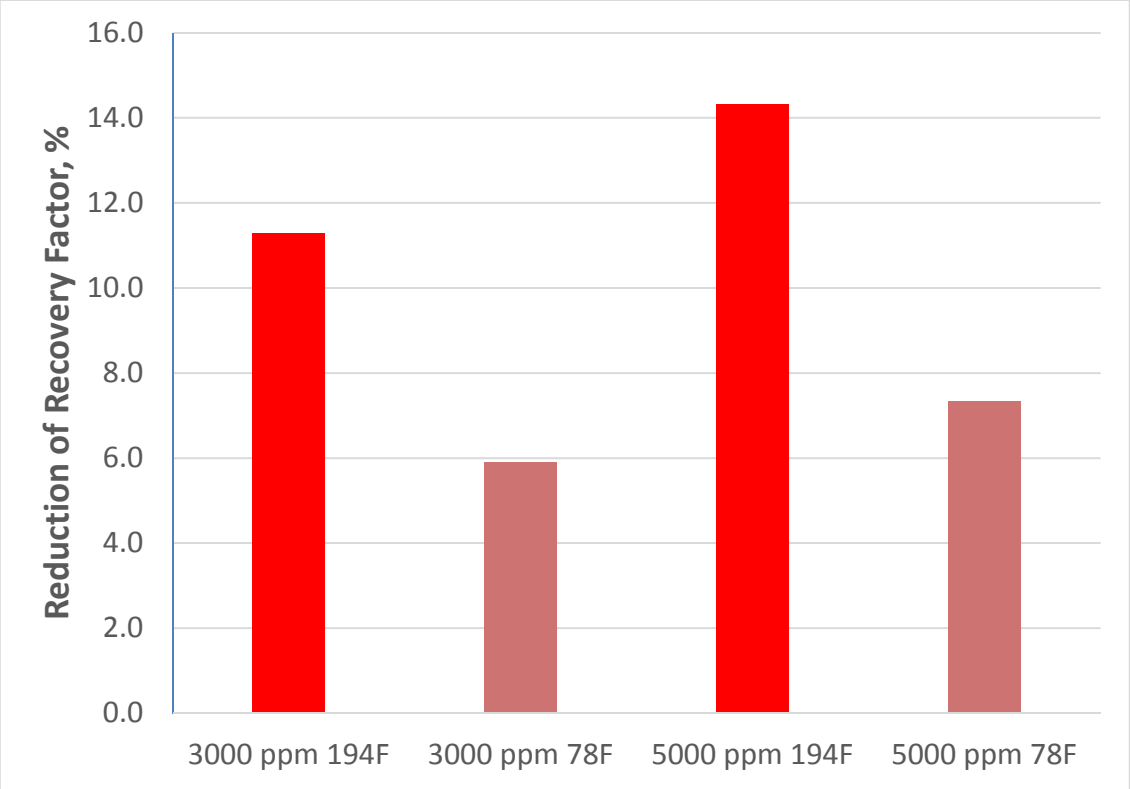

Figure 4.6: Reduction of recovery factor due to degradation.

The final recovery factor are also shown in **Figure 4.7**. With the injection temperature of 194°F, when polymer concentration is increased from 3000 ppm to 5000 ppm, the incremental oil recovery is 0.7%. On the other hand, with the injection temperature of 78°F, when polymer concentration is increased from 3000 ppm to 5000 ppm, the incremental oil recovery is 1.8%. This demonstrates that if we want to increase polymer concentration to obtain higher recovery factor, higher injection temperature will make this method less efficient.

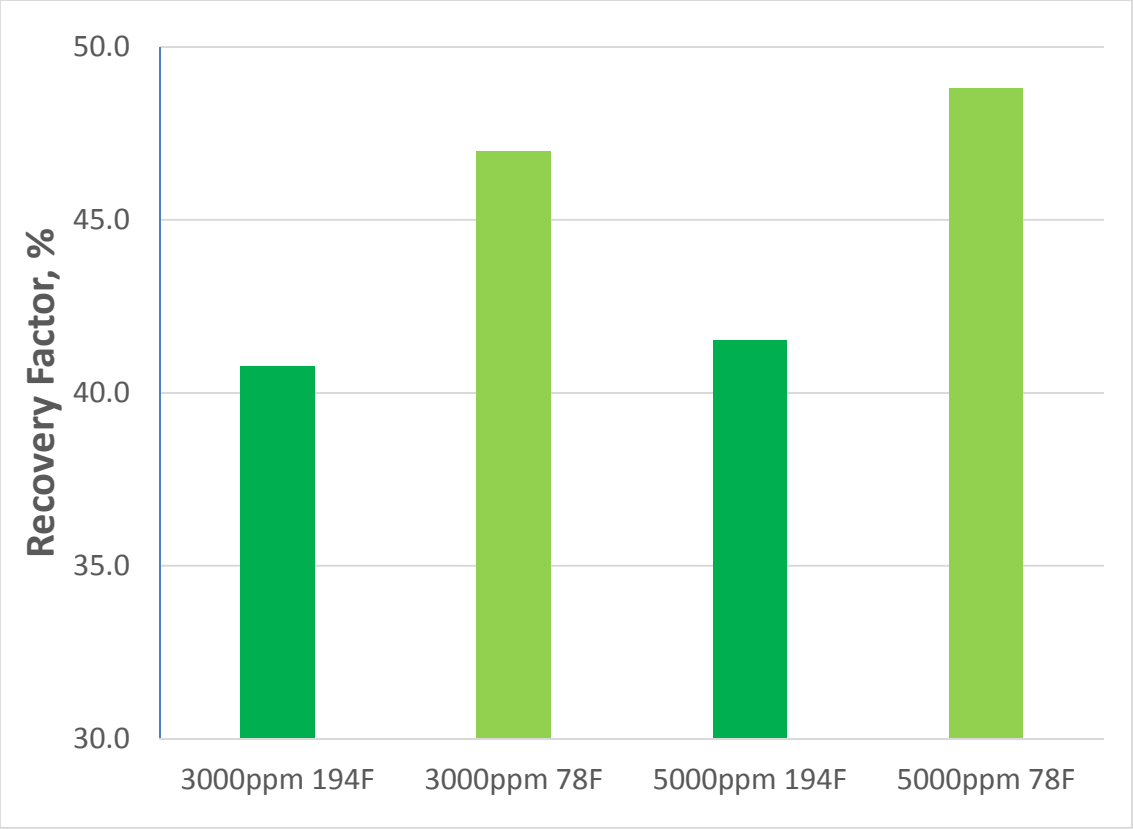

Figure 4.7: Recovery factor of polymer flood at different concentration and temperature with degradation.

4.4 Summary

After the literature survey and simulation study, the following conclusion can be drawn:

1. High temperature accelerates the polymer degrade, resulting in loss of viscosity and low incremental recovery factor.

2. When temperature is high, even more polymer is injected to maintain high viscosity during flood process, degradation makes the additional polymer useless.

5. WATER SHUTOFF AND IN-DEPTH PROFILE CONTROL

5.1 Background

High temperature is a favorable condition for the application of in-depth profile control. A weak gel system used as a nontarget in-depth profile control is modeled to study its potential for enhancement of polymer flood. As a comparison, the recovery effect of water shutoff is also studied. To realize the actual condition, polymer retention effect is included.

5.2 Simulation Input Description

Because water shutoff is a process to seal high permeability layers at near well region, so it is simulated as shutting in both injector and producers at high permeability layer. The effect is like there is no perforation on the wells at the third layer.

Polymer flood with concentration of 3000 ppm is also simulated, including the degradation and retention effect. The modeling of retention is discussed in the following section.

5.3 Polymer Retention Modelling

The Langmuir adsorption isotherm is used to model the polymer retention, as mentioned in **2.4.4**. The maximum adsorption capacity is $3.38*10^{-8}$ lbmol/ft^3. The residual adsorption level is set to the same value to model irreversible retention. Parameters of

Langmuir isotherm are set as tad1=16.3 lbmol/ft^3, tad2=0, and tad3= 3.12149*10^8. The resistance factor of polymer is 1.2 for all the rock.

5.4 Simulation Studies of Resistance Caused by Polymer Retention

Result shows that maximum adsorption of 3.38*10^{-8} lbmol/ft^3 is quickly reached after polymer injected (**Figure 5.1**). Because the fluid flow rate is higher in layers with higher permeability, so more polymer are trapped on the rock there. The adsorbed polymer causes resistance to water phase flow (**Figure 5.2**).

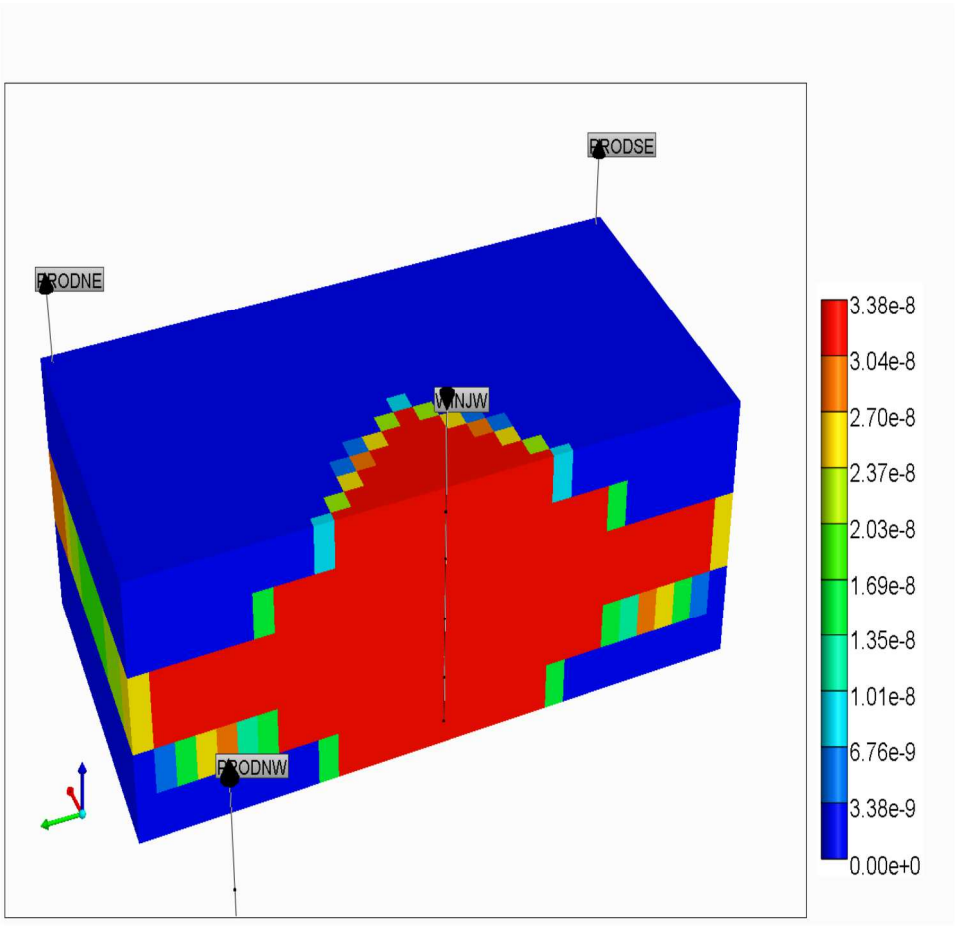

Figure 5.1: Polymer adsorption (lb/ft^3) at the beginning of polymer flood.

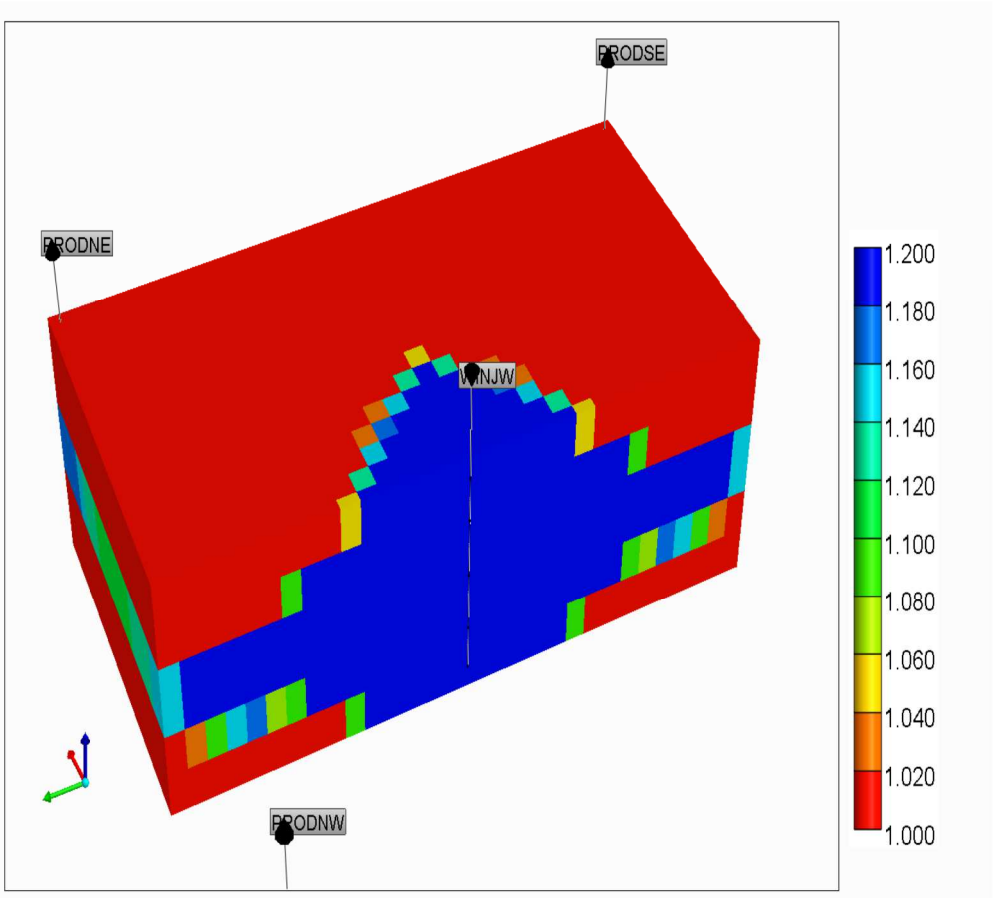

Figure 5.2: Resistance factor changes due to polymer adsorption.

Resistance to water flow will decrease the mobility of water, resulting in the decrease of water cut and increase of final oil recovery (1.2%). Generally, retention of polymer does not affect the oil recovery performance significantly (**Figure 5.3**). It is because the sandstone surface does not adsorb a large amount of polymer, which does not obviously influence polymer solution viscosity. On the other hand, the adsorbed polymer cannot make strong resistance to water phase flow, contributing little in improving mobility ratio.

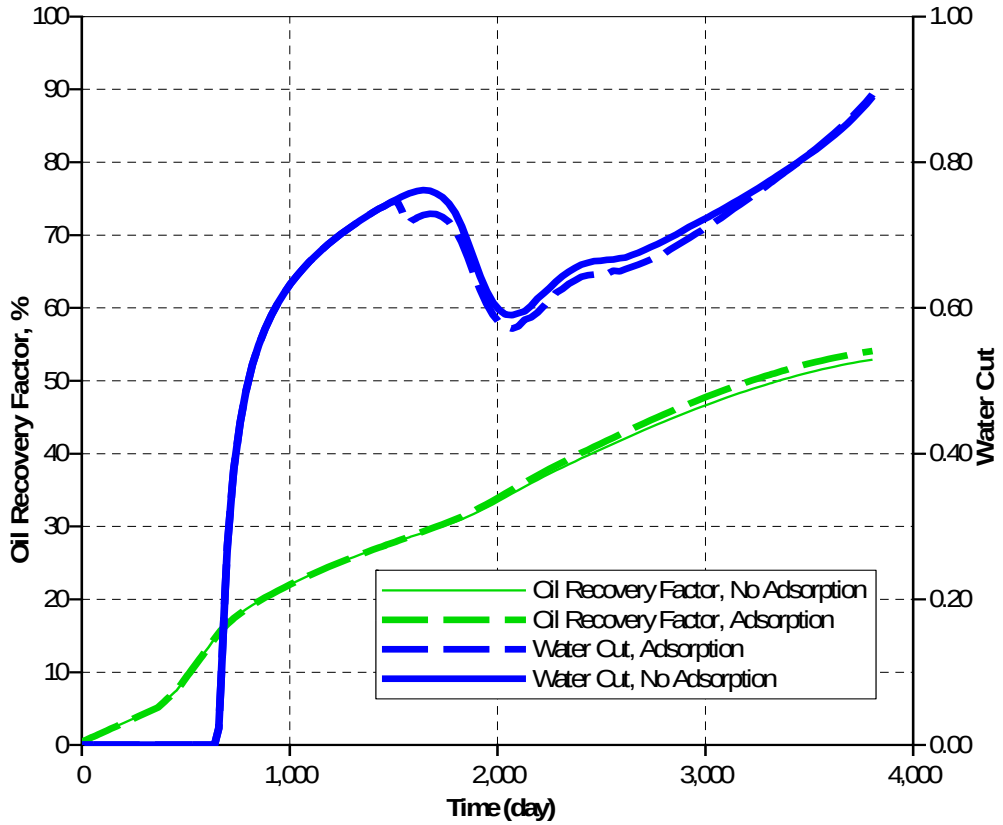

Figure 5.3: Oil recovery factors and water cut of polymer flood with adsorption effects and without adsorption effects.

5.5 Comparison of Water Shutoff, In-Depth Profile Control, and the Combination of In-Depth Profile Control and Polymer Flood

4 cases in total were run for the comparison. All the cases have the same pre-flush slug of 0.33 PV and the same total injection of 1.03 PV. The reservoir temperature is 194°F. For water shutoff case, the injection temperature is 78°F. After pre-flush, the production and injection at high permeability layer were shut in, while the injection and production rate is kept same as before. For in-depth profile control cases, two injection temperature were tested: 78°F and 194°F. After pre-flush, 3000 ppm polymer and 850 ppm crosslinker were injected simultaneously for 0.018 PV, followed by 0.68 PV post

waterflood. For the combination of in-depth profile control and polymer flood case, the injection temperature is 78°F. After the profile control slug of 0.018 PV, a chasing polymer flood followed for 0.54 PV. The polymer slug size is same as that in the simple polymer flood in **5.3**. After polymer flood, a post waterflood of 0.14 PV was injected to keep the total injection pore volume as same as that in other cases (**Figure 5.4**).

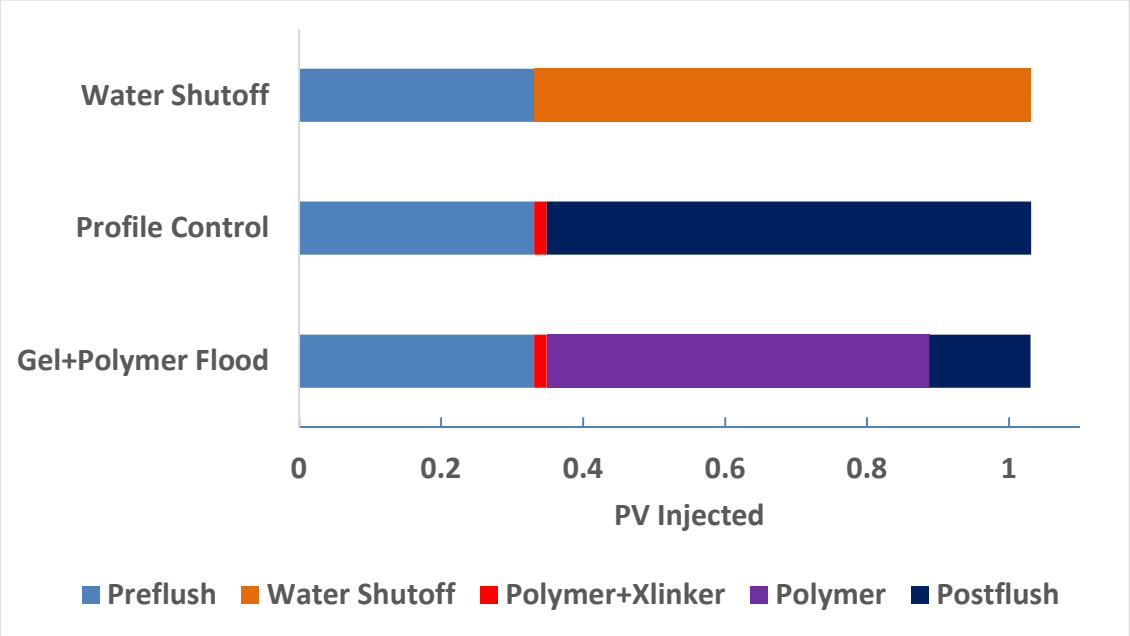

Figure 5.4: Injection scheme of water shutoff case, in-depth profile control case, and combination of in-depth profile control and polymer flood case.

Simulation result indicates that water shutoff can increase the final recovery factor by 5.3%. It also shows that after implementation of water shutoff, water cut largely decreases immediately. But it increases sharply after a short while (**Figure 5.5**). The reason is that although the high permeability layer is sealed at the near well region, cross flow occurs at deep reservoir, which makes high permeability layer to become a water

channel. It allows flow injected and produced in lower permeability region to pass through. This phenomena is shown as change of water saturation in **Figure 5.6**.

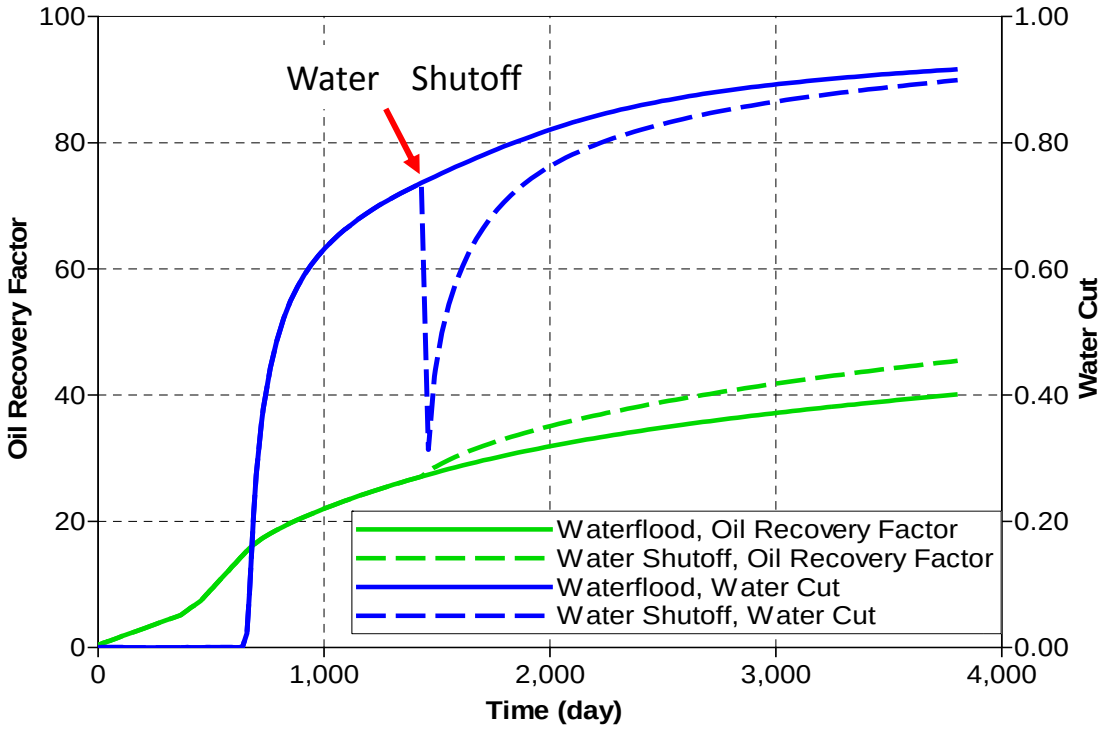

Figure 5.5: Oil recovery factor and water cut of waterflood case and water shutoff case.

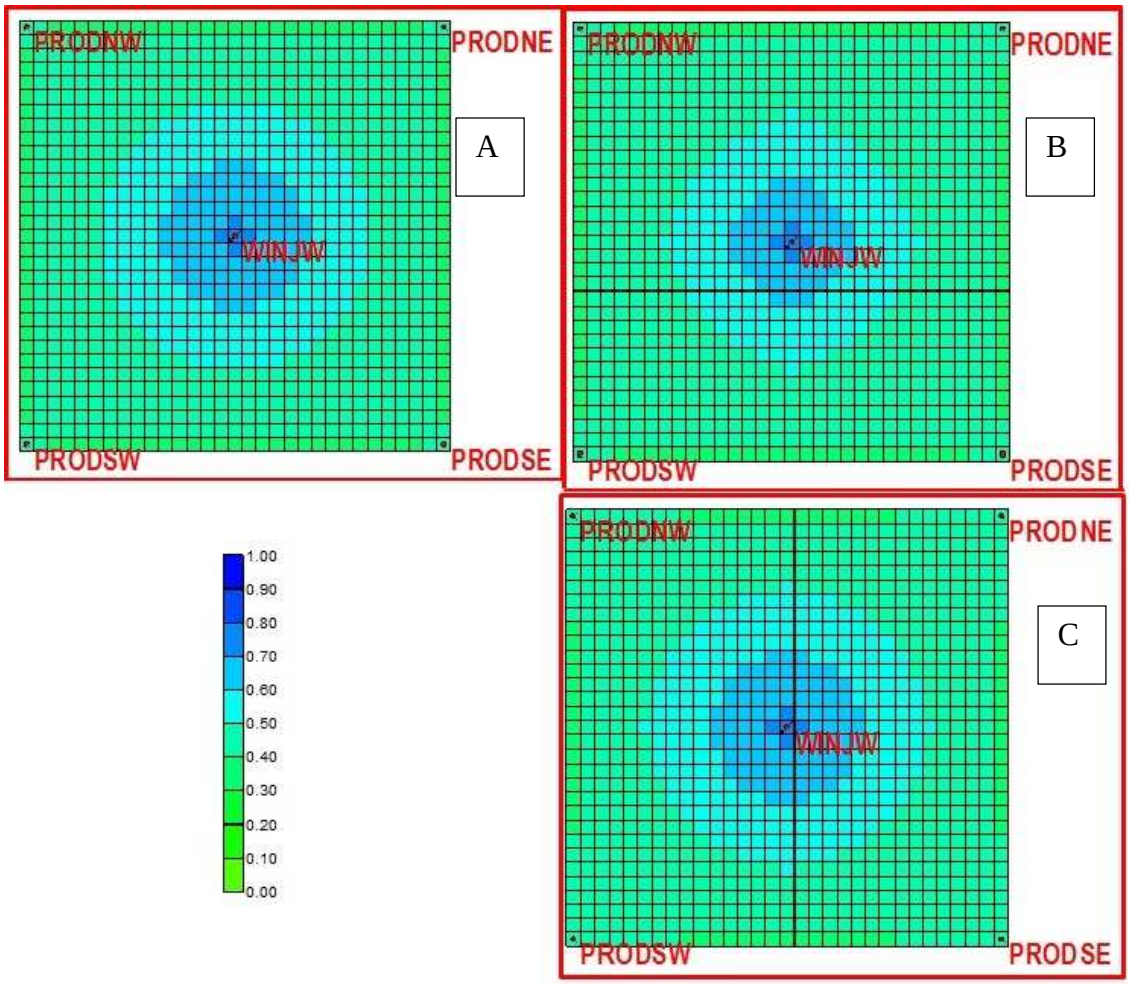

Figure 5.6: Change of water saturation at high perm layer. A: Beginning of water shutoff. B: 5 months later. Water saturation decreases because oil from neighbor layers is driven to this layer. C: 1.5 years later. Water saturation increases because connection between layers make it to be a water channel again.

The function of gel as an in-depth profile control chemical is realized as its adsorption on rock to resist water phase flow in this study. The Langmuir adsorption isotherm is used to model the gel adsorption. The maximum adsorption capacity is 0.0276 lbmol/ft^3. The residual adsorption level is set to the same value to model irreversible adsorption. Parameters of Langmuir isotherm are set as tad1=276 lbmol/ft^3, tad2=0, and

tad3= 10,000. The resistance factor of polymer is 19.25 for all the rock. All adsorption parameters except resistance factor are obtained from CMG example case. The resistance factor is calculated from literature (Al-Muntasheri et al. 2007; Al-Muntasheri et al. 2008; Al-Muntasheri et al. 2009).

For in-depth profile control cases, the incremental recovery factor for 78°F injection temperature is 7.4%, which is higher than that for 194°F injection temperature, 3.3%. The reason is that different temperature field causes different gel production and distribution. With 78°F injection temperature, the temperature at near well region is low, which is an unfavorable condition for gelation reaction. When the slug of polymer and crosslinker propagates to deep reservoir, high temperature there accelerates the reaction. So more gel is distributed at deep reservoir in high permeability layers (**Figure 5.7**), which weakens the water crossflow there. With 194°F injection temperature, the temperature at near well region is high, thus most of the gel is produced and assemble there. Severe crossflow still occurs from low permeability layers to high permeability layers in deep reservoir (**Figure 5.8**). Fluid production rate at high permeability layer also demonstrate that more amount gel distributed at deep reservoir leads to a better sealing effect (**Figure 5.9**). After injection of polymer and crosslinker slug, for 78°F case, production rate at high permeability layer decreases, while for 194°F case, production rate does not has obvious change.

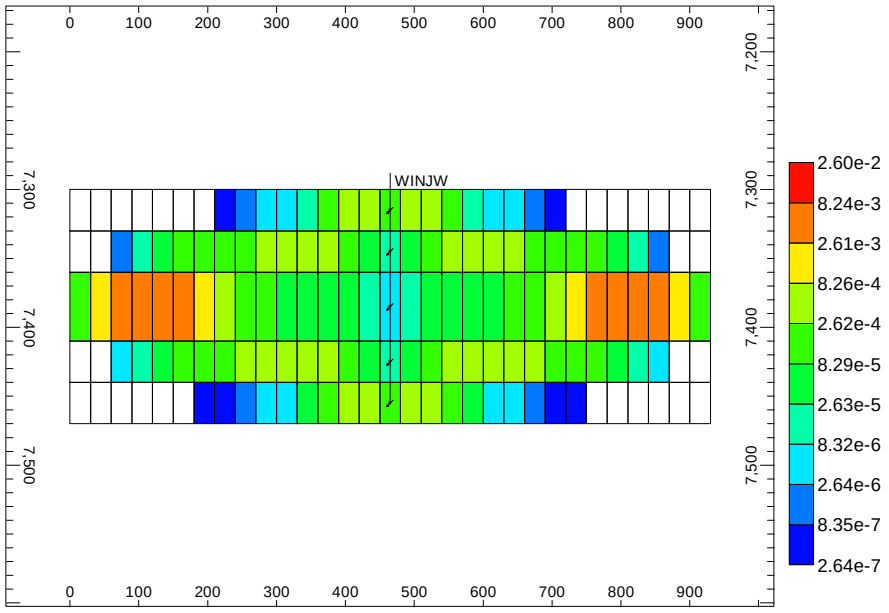

Figure 5.7: Injector cross-section profile shows the amount of gel adsorbed on the rock with injection temperature of 78°F.

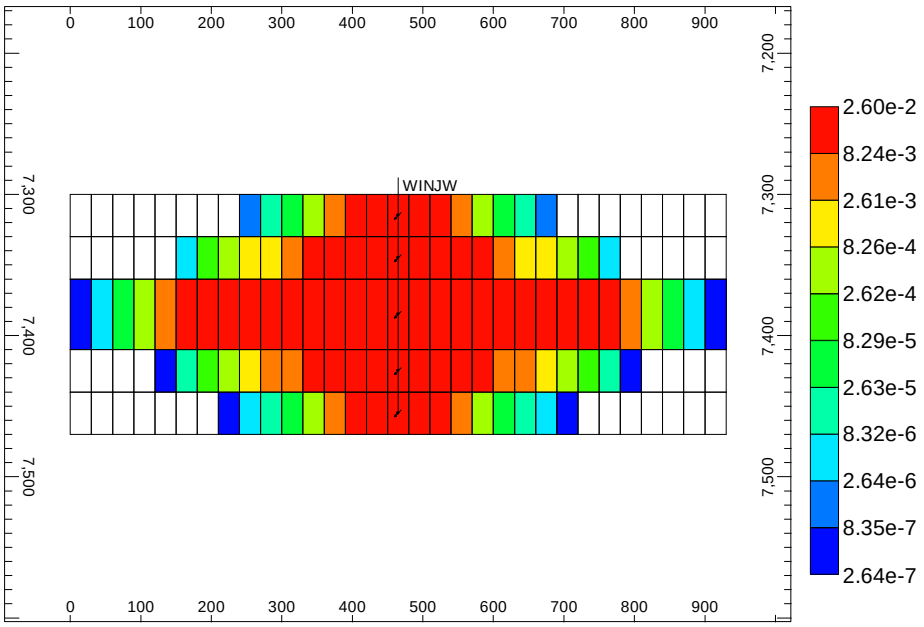

Figure 5.8: Injector cross-section profile shows the amount of gel adsorbed on the rock with injection temperature of 194°F.

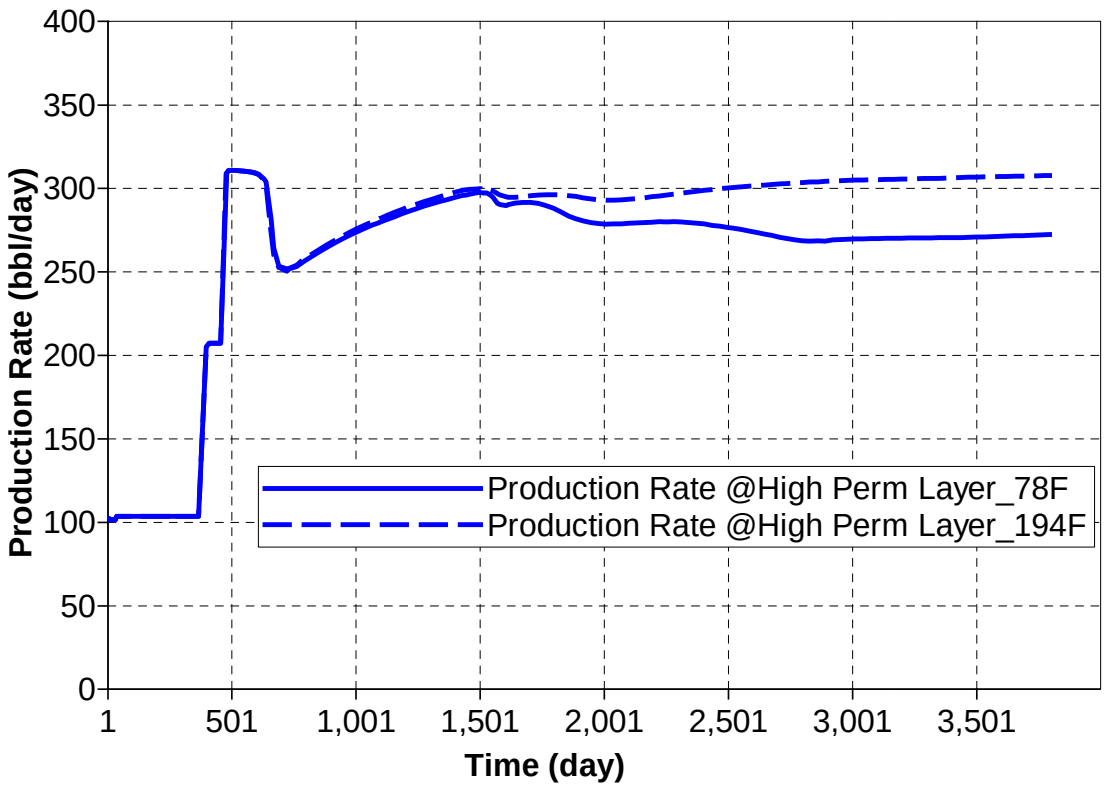

Figure 5.9: Liquid production rate at high permeability layer of one producer.

High injection temperature may also cause injectivity problem, because plenty of gel seals injection flow at near well region. For injection temperature of 78°F, the injection pressure increases to 1.7 times of its initial during gel reactants injection, and keeps to 1.03 times of its initial during the followed waterflood. For injection temperature of 194°F, the injection pressure increases to 3.7 times of its initial during gel reactants injection, and keeps to 1.4 times of its initial during the followed waterflood (**Figure 5.10**).

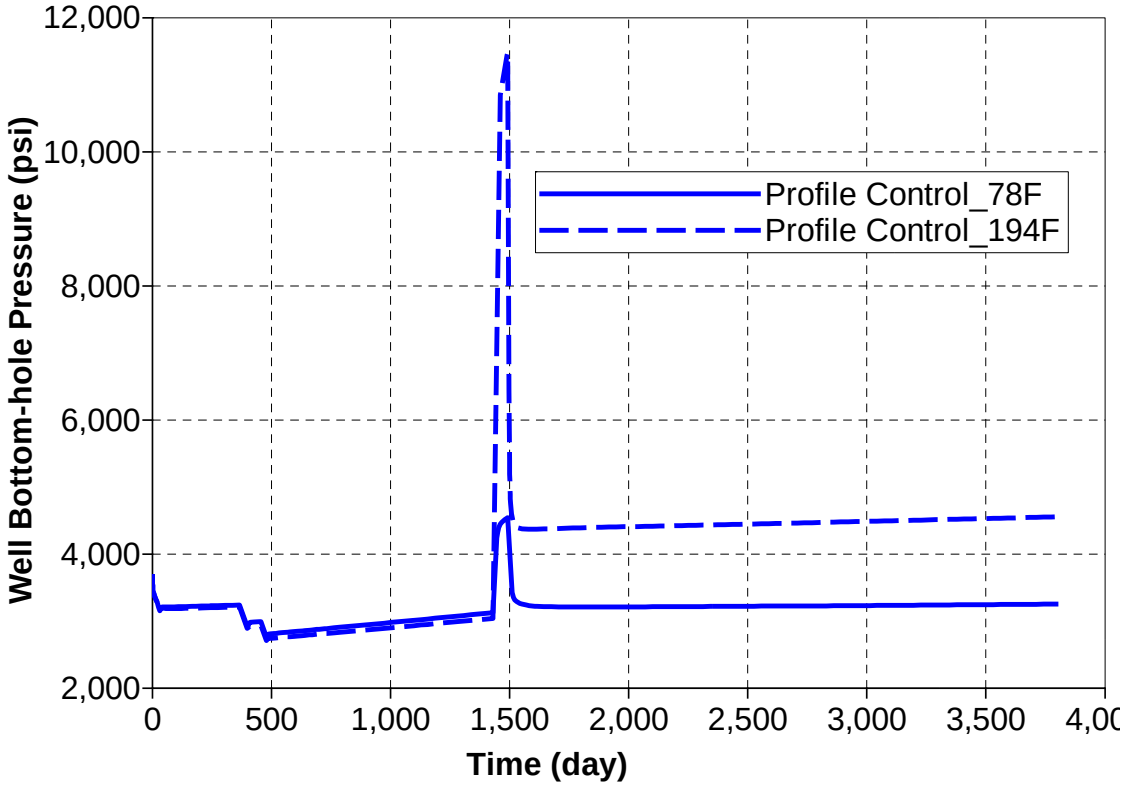

Figure 5.10: Injection pressure for in-depth profile control cases with injection temperature of 78°F and 194°F.

Oil recovery performance of the combination of in-depth profile control and polymer flood is simulated, and compared to waterflood, water shutoff, simple in-depth profile control and simple polymer flood. For all the cases, the reservoir temperature is 194°F, and injection temperature is 78°F. The incremental oil recovery factor for the combination method is the highest (14.3%), and it is even higher than the sum of incremental oil recovery factors of simple in-depth profile control (7.4%) and simple polymer flood (5.9%). Additionally, there's still potential for more oil recovery for the

combination method, because the water cut at the end of process is the lowest, compared to other methods (**Figure 5.12**).

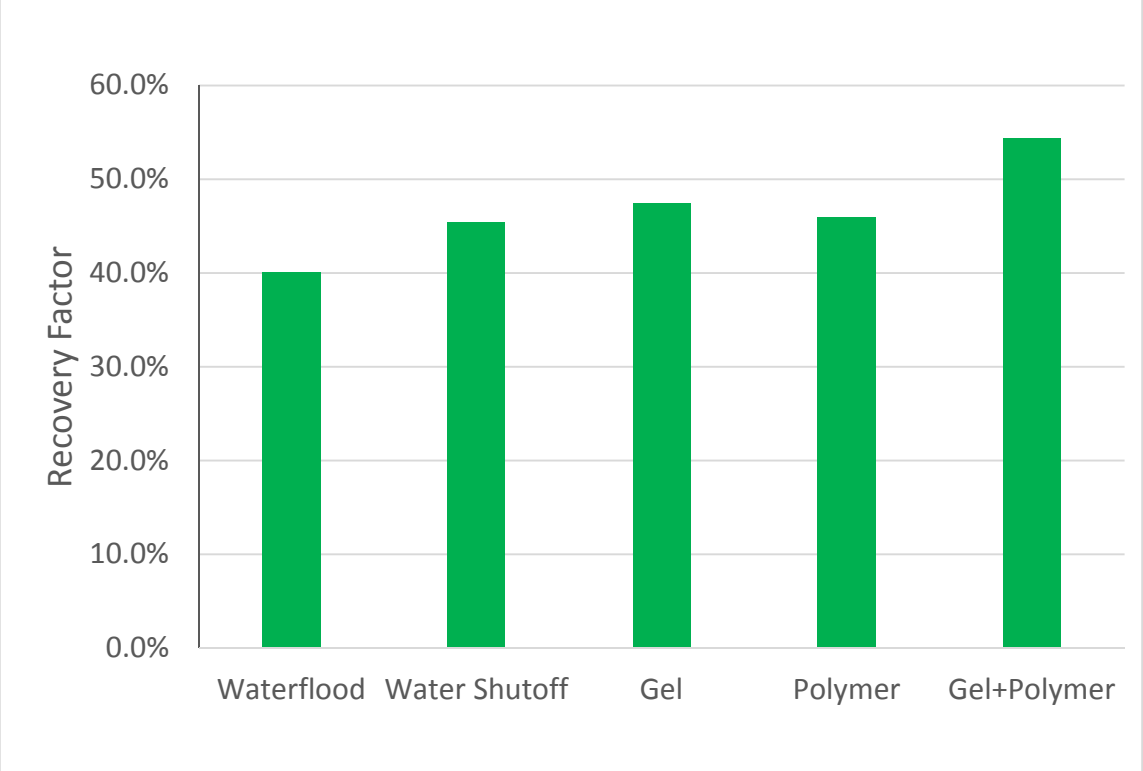

Figure 5.11: Recovery factor of waterflood case, water shutoff case, in-depth profile control case, 3000 ppm polymer flood case, and the combination application of in-depth profile control and 3000 ppm polymer flood case.

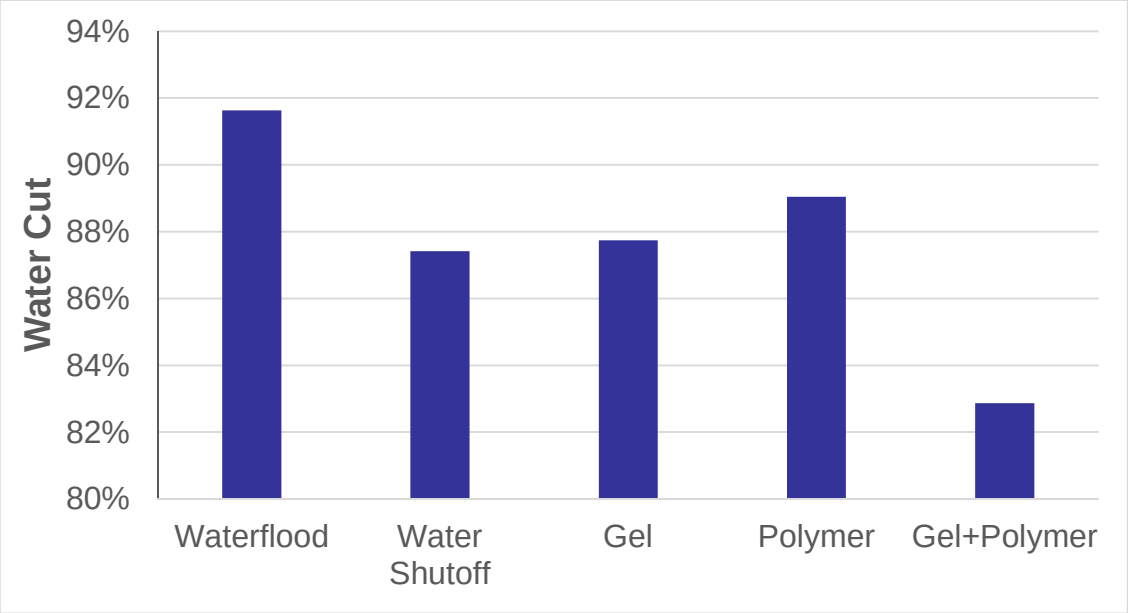

Figure 5.12: Water cut at the end of the process of waterflood case, water shutoff case, in-depth profile control case, 3000 ppm polymer flood case, and the combination application of in-depth profile control and 3000 ppm polymer flood case.

5.6 Summary

Polymer adsorption was modeled and the assistant methods to polymer flood such as water shutoff and in-depth profile control were studied. Based on the results obtained, the following conclusions can be drawn:

1. Polymer adsorption slightly increases the final recovery factor, due to its resistance to water phase flow.

2. Water shutoff can increase the final recovery factor, but crossflow still occurs in deep reservoir.

3. Lower injection temperature is preferred for application of in-depth profile control, because it can make more gel distributed in deep reservoir.

4. In terms of final recovery factor and water cut, the combination method of in-depth profile control and polymer flood has the best recovery performance.

6. CONCLUSIONS AND RECOMMENDATIONS

In the aspect of polymer thermal thinning, high temperature has no obvious effect on oil recovery. It is because the change of mobility ratio of displacing fluid and displaced fluid is marginal. But considering polymer thermal degradation and gel distribution, injection fluid with lower temperature is preferred, which can defer the polymer degradation, and build favorable temperature gradient for gelation.

Both near-well water shutoff and in-depth profile control can improve waterflood. However in-depth profile control will help polymer flood be more efficient without causing severe injectivity problem. Thus the combination of in-depth profile control and polymer flood achieves the highest recovery performance in high temperature reservoir.

REFERENCES

Afsharpoor, A., Ma, K., Duboin, A. et al. 2014. Micro-Scale Experiment and CFD Modeling of Viscoelastic Polymer; Trapped Oil Displacement and Deformation at the Dead-End. Paper presented at the the SPE Improved Oil Recovery Symposium, Tulsa, Oklahoma, USA, 12–16 April 2014. SPE 169037. DOI: 10.2118/169037-MS.

Al-Adasani, A. and Bai, B. 2010. Recent Developments and Updated Screening Criteria of Enhanced Oil Recovery Techniques. Paper presented at the the CPS/SPE International Oil & Gas Conference and Exhibition in China, Beijing, China, 8–10 June 2010. SPE 130726. DOI: 10.2118/130726-MS.

Al-Muntasheri, G.A., Nasr-El-Din, H.A., Al-Noaimi, K. et al. 2009. A Study of Polyacrylamide-Based Gels Crosslinked with Polyethyleneimine. *SPE Journal* **14** (02): 245-251. DOI: 10.2118/105925-PA

Al-Muntasheri, G.A., Nasr-El-Din, H.A., and Zitha, P.L.J. 2008. Gelation Kinetics and Performance Evaluation of an Organically Crosslinked Gel at High Temperature and Pressure. *SPE Journal* **13** (03): 337-345. DOI: 10.2118/104071-PA

Al-Muntasheri, G.A., Zitha, P.L.J., and Nasr-El-Din, H.A. 2007. Evaluation of a New Cost-Effective Organic Gel System for High Temperature Water Control. Paper presented at the the International Petroleum Technology Conference, Dubai, U.A.E., 4–6 December 2007. IPTC 11080. DOI: 10.2523/11080-MS.

Al-Shammari, B., Al-Fariss, T., Al-Sewailm, F. et al. 2011. The Effect of Polymer Concentration and Temperature on the Rheological Behavior of Metallocene

Linear Low Density Polyethylene (Mlldpe) Solutions. *Journal of King Saud University - Engineering Sciences* **23** (1): 9-14. DOI: http://dx.doi.org/10.1016/j.jksues.2010.07.001

Bataweel, M.A. 2011. Enhanced Oil Recovery in High Salinity High Temperature Reservoir by Chemical Flooding. 3500160 Ph.D., Texas A&M University.

Brown, C.E., Christie, M.A., and Gatt, A.M. 1982. Reservoir Temperature Distributions around Injection Wells: Effect on EOR Schemes. In *Proc*:253-261.

Choi, B., Lee, K.S., and Yu, K. 2014. Permeability-Dependent Retention of Polymer in Heterogeneous Reservoirs. Paper presented at the the Offshore Technology Conference Asia, Kuala Lumpur, Malaysia, 25–28 March 2014. OTC 24880. DOI: 10.2118/24880-MS.

Clifford, P.J. and Sorbie, K.S. 1985. The Effects of Chemical Degradation on Polymer Flooding. Paper presented at the the International Symposium on Oilfield and Geothemral Chemistry, Phoenix, Arizona, April 9-11, 1985. SPE 13586. DOI: 10.2118/13586-MS.

Dawkrajai, P., Lake, L.W., Yoshioka, K. et al. 2006. Detection of Water or Gas Entries in Horizontal Wells from Temperature Profiles. Paper presented at the the 2006 SPE/DOE Symposium on Improved Oil Recovery, Tulsa, Oklahoma, U.S.A., 22–26 April 2006. SPE 100050. DOI: 10.2118/100050-MS.

Dong, H., Fang, S., Wang, D. et al. 2008. Review of Practical Experience & Management by Polymer Flooding at Daqing. Paper presented at the the 2008 SPE/DOE

Improved Oil Recovery Symposium, Tulsa, Oklahoma, U.S.A., 19–23 April 2008. SPE 114342. DOI: 10.2118/114342-MS.

Fernandez, I.J. 2005. Evaluation of Cationic Water-Soluble Polymers with Improved Thermal Stability. Paper presented at the the 2005 SPE International Symposium on Oilfield Chemistry, Houston, Texas, U.S.A., 2 – 4 February 2005. SPE 93003. DOI: 10.2118/93003-MS.

Gaillard, N., Giovannetti, B., Favero, C. et al. 2014. New Water Soluble Anionic Nvp Acrylamide Terpolymers for Use in Harsh EOR Conditions. Paper presented at the the SPE Improved Oil Recovery Symposium, Tulsa, Oklahoma, USA, 12–16 April 2014. SPE 169108. DOI: 10.2118/169108-MS.

Gaillard, N., Sanders, D.B., and Favero, C. 2010. Improved Oil Recovery Using Thermally and Chemically Protected Compositions Based on Co- and Ter-Polymers Containing Acrylamide. Paper presented at the the 2010 SPE Improved Oil Recovery Symposium, Tulsa, Oklahoma, USA, 24–28 April 2010. SPE 129756. DOI: 10.2118/129756-MS.

Gao, C.H. 2014. Experiences of Polymer Flooding Projects at Shengli Oilfield. Paper presented at the the SPE EOR Conference at Oil and Gas West Asia, Muscat, Oman, 31 March–2 April 2014. SPE 169652. DOI: 10.2118/169652-MS.

Goudarzi, A., Delshad, M., and Sepehrnoori, K. 2013. A Critical Assessment of Several Reservoir Simulators for Modeling Chemical Enhanced Oil Recovery Processes. Paper presented at the the SPE Reservoir Simulation Symposium, Woodlands, Texas, USA, 18-20 February 2013. SPE 163578. DOI: 10.2118/163578-MS.

Han, M., Zhou, X., Alhasan, F.B. et al. 2012. Laboratory Investigation of the Injectivity of Sulfonated Polyacrylamide Solutions into Carbonate Reservoir Rocks. Paper presented at the the SPE EOR Conference at Oil and Gas West Asia, Muscat, Oman, 16–18 April 2012. SPE 155390. DOI: 10.2118/155390-MS.

He, J., Song, Z., Qiu, L. et al. 1998. High Temperature Polymer Flooding in Thick Reservoir in Shuanghe Oilfield. Paper presented at the the 1998 SPE Intemationa Conference and Exhibition in China Beijing, 2-6 November 1998. SPE 50933. DOI: 10.2118/50933-MS.

Hsieh, H., Moradi‐Araghi, A., Stahl, G. et al. 1992. Water‐Soluble Polymers for Hostile Environment Enhanced Oil Recovery Applications. In *Makromolekulare Chemie. Macromolecular Symposia*, 64:121-135: Wiley Online Library.ISBN 1521-3900.

Huh, C. and Pope, G.A. 2008. Residual Oil Saturation from Polymer Floods: Laboratory Measurements and Theoretical Interpretation. Paper presented at the the 2008 SPE/DOE Improved Oil Recovery Symposium, Tulsa, Oklahoma, U.S.A., 19–23 April 2008. SPE 113417. DOI: 10.2118/113417-MS.

Ikegami, A. and Imai, N. 1962. Precipitation of Polyelectrolytes by Salts. *Journal of Polymer Science* **56** (163): 133-152.

Kang, P.-S., Lim, J.-S., and Huh, C. 2013. A Novel Approach in Estimating Shear-Thinning Rheology of Hpam and Amps Polymers for Enhanced Oil Recovery Using Artificial Neural Network. Paper presented at the the Twenty-third (2013)

International Offshore and Polar Engineering, Anchorage, Alaska, USA, June 30–July 5, 2013. International Society of Offshore and Polar Engineers.

Khan, M.Y., Samanta, A., Ojha, K. et al. 2009. Design of Alkaline/Surfactant/Polymer (Asp) Slug and Its Use in Enhanced Oil Recovery. *Petroleum Science and Technology* **27** (17): 1926-1942. DOI: 10.1080/10916460802662765

Lake, L.W. 2010. *Enhanced Oil Recovery*. Richardson, Texas: Society of Petroleum Engineers. Original edition. ISBN.

Lee, K.S. 2011. Performance of a Polymer Flood with Shear-Thinning Fluid in Heterogeneous Layered Systems with Crossflow. *Energies* **4** (8): 1112-1128.

Lee, S., Kim, D.H., Huh, C. et al. 2009. Development of a Comprehensive Rheological Property Database for EOR Polymers. Paper presented at the the 2009 SPE Annual Technical Conference and Exhibition, New Orleans, Louisiana, USA, 4–7 October 2009. SPE 124798. DOI: 10.2118/124798-MS.

Levitt, D. and Pope, G.A. 2008. Selection and Screening of Polymers for Enhanced-Oil Recovery. Paper presented at the the 2008 SPE/DOE Improved Oil Recovery Symposium, Tulsa, Oklahoma, U.S.A., 19–23 April 2008. SPE 113845. DOI: 10.2118/113845-MS.

Liu, H., Li, J., Yan, J. et al. 2009. Successful Practices and Development of Polymer Flooding in Daqing Oilfield. Paper presented at the the 2009 SPE Asia Pacific Oil and Gas Conference and Exhibition, Jakarta, Indonesia, 4–6 August 2009. SPE 123975. DOI: 10.2118/123975-MS.

Lu, Y. 1994. A Study of Residual Oil Saturation in Heterogeneous Sandstone Experiments, University of Texas at Austin.

Moore, J.K. 1969. Reservoir Barrier and Polymer Waterflood, Northeast Hallsville Crane Unit. *Journal of Petroleum Technology* **21** (09): 1130-1136. DOI: 10.2118/2423-PA

Nasr-El-Din, H.A., Bitar, G.E., Bou-Khamsin, F.I. et al. 1998. Field Application of Gelling Polymers in Saudi Arabia. Paper presented at the the 1998 SPE/DOE Improved Oil Recovery Symposium Tulsa, Oklahema, 19-22 April 1998. SPE 39615. DOI: 10.2118/39615-MS.

Nasr-El-Din, H.A., Hawkins, B.F., and Green, K.A. 1991. Viscosity Behavior of Alkaline, Surfactant, Polyacrylamide Solutions Used for Enhanced Oil Recovery. Paper presented at the the SPE International Symposium on Oilfield Chemistry, Anaheim, California, February 20-22, 1991. SPE 21028. DOI: 10.2118/21028-MS.

Okeke, T. and Lane, R.H. 2012. Simulation and Economic Screening of Improved-Conformance Oil Recovery by Polymer Flooding and a Thermally Activated Deep Diverting Gel. Paper presented at the the SPE Western Regional Meeting, Bakersfield, California, USA, 19–23 March 2012. SPE 153740. DOI: 10.2118/153740-MS.

Pederson, J.M. and Sitorus, J.H. 2001. Geothermal Hot-Water Flood -Balam South Telisa Sand, Sumatra, Indonesia. Paper presented at the the SPE Asia Pacific Oil and Gas

Conference and Exhibition, Jakarta, Indonesia, 17-19 April 2001. SPE 68724. DOI: 10.2118/68724-MS.

Putz, A.G., Lecourtier, J.M., and Bruckert, L. 1988. Interpretation of High Recovery Obtained in a New Polymer Flood in the Chateaurenard Field. Paper presented at the the 62rd Annual Technical Conference and Exhibition of the Societyof Petroleum Engineers, Houston,TX, October 2-5, 1988. SPE 18093. DOI: 10.2118/18093-MS.

Saleh, L.D., Wei, M., and Bai, B. 2014. Data Analysis and Updated Screening Criteria for Polymer Flooding Based on Oilfield Data. *SPE Reservoir Evaluation & Engineering* **17** (01): 15-25. DOI: 10.2118/168220-PA

Schramm, L.L. 2000. *Surfactants: Fundamentals and Applications in the Petroleum Industry*. Cambridge, United Kingdom: Cambridge University Press. Original edition. ISBN 0521640679.

Seright, R., Zhang, G., Akanni, O. et al. 2012. A Comparison of Polymer Flooding with in-Depth Profile Modification. *Journal of Canadian Petroleum Technology* **51** (05): 393-402. DOI: 10.2118/146087-PA

Sorbie, K.S. and Clifford, P.J. 1988. The Simulation of Polymer Flow in Heterogeneous Porous Media. In *Water-Soluble Polymers for Petroleum Recovery*, ed. Stahl, G.A. and Schulz, D.N.: Springer US.

Sorbie, K.S., Roberts, L.J., and Foulser, R.W.S. 1982. Polymer Flooding Calculations for Highly Stratified Brent Sands in the North Sea. In *the 2nd European Symposium on EOR*:175-190. Paris, France, 8–10 November.

Sorbie, K.S. and Seright, R.S. 1992. Gel Placement in Heterogeneous Systems with Crossflow. Paper presented at the the SPE/DOE Eighth Symposium on Enhanced Oil Recovery, Tulsa. Oklahoma, April 22-24, 1992. SPE 24192. DOI: 10.2118/24192-MS.

Vela, S., Peaceman, D.W., and Sandvik, E.I. 1976. Evaluation of Polymer Flooding in a Layered Reservoir with Crossflow, Retention, and Degradation. *SPE Journal* **16** (02): 82-96. DOI: 10.2118/5102-PA

Vermolen, E.C.M., Van Haasterecht, M.J.T., Masalmeh, S.K. et al. 2011. Pushing the Envelope for Polymer Flooding Towards High-Temperature and High-Salinity Reservoirs with Polyacrylamide Based Ter-Polymers. Paper presented at the the SPE Middle East Oil and Gas Show and Conference, Manama, Bahrain, 25–28 September 2011. SPE 141497. DOI: 10.2118/141497-MS.

Wang, D., Xia, H., Liu, Z. et al. 2001. Study of the Mechanism of Polymer Solution with Visco-Elastic Behavior Increasing Microscopic Oil Displacement Efficiency and the Forming of Steady "Oil Thread" Flow Channels. Paper presented at the the SPE Asia Pacific Oil and Gas Conference and Exhibition, Jakarta, Indonesia, 17–19 April 2001. SPE 68723. DOI: 10.2118/68723-MS.

Wreath, D.G. 1989. A Study of Polymer Flooding and Residual Oil Saturation, University of Texas at Austin.

Wu, X., Sui, W., and Jiang, Y. 2013. Innovative Applications of Downhole Temperature Data. Paper presented at the the SPE Middle East Intelligent Energy Conference

and Exhibition, Dubai, UAE, 28–30 October 2013. SPE 167477. DOI: 10.2118/167477-MS.

Xia, H., Wang, D., Wu, J. et al. 2004. Elasticity of Hpam Solutions Increases Displacement Efficiency under Mixed Wettability Conditions. Paper presented at the the SPE Asia Pacific Oil and Gas Conference and Exhibition, Perth, Australia, 18–20 October 2004. SPE 88456. DOI: 10.2118/88456-MS.

Yoshioka, K., Zhu, D., Hill, A.D. et al. 2007. Prediction of Temperature Changes Caused by Water or Gas Entry into a Horizontal Well. DOI: 10.2118/100209-pa

Zaitoun, A. and Potie, B. 1983. Limiting Conditions for the Use of Hydrolyzed Polyacrylamides in Brines Containing Divalent Ions. Paper presented at the the International Symposium on Oilfield and Geothermal Chemistry, Denver, CO,. June 1-3, 1983. SPE 11785. DOI: 10.2118/11785-MS.